

1 **Title**

2 Aversive experience drives offline ensemble reactivation to link memories across days

3

4

5 **Authors**

6 Yosif Zaki<sup>1</sup>, Zachary T. Pennington<sup>1</sup>, Denisse Morales-Rodriguez<sup>1</sup>, Taylor R. Francisco<sup>1</sup>, Alexa R.  
7 LaBanca<sup>1</sup>, Zhe Dong<sup>1</sup>, Sophia Lamsifer<sup>1</sup>, Simón Carrillo Segura<sup>2</sup>, Hung-Tu Chen<sup>4</sup>, Zoé Christenson  
8 Wick<sup>1</sup>, Alcino J. Silva<sup>3</sup>, Matthijs van der Meer<sup>4</sup>, Tristan Shuman<sup>1</sup>, André Fenton<sup>5,6</sup>, Kanaka Rajan<sup>1</sup>,  
9 Denise J. Cai<sup>1\*</sup>

10

11 <sup>1</sup>Nash Department of Neuroscience, Icahn School of Medicine at Mount Sinai, New York, NY, 10029

12 <sup>2</sup>Graduate Program in Mechanical and Aerospace Engineering, Tandon School of Engineering, New  
13 York University, Brooklyn, NY, 11201

14 <sup>3</sup>Department of Neurobiology, Psychiatry & Biobehavioral Sciences, and Psychology, Integrative Center  
15 for Learning and Memory, Brain Research Institute, UCLA, Los Angeles, CA 90095

16 <sup>4</sup>Department of Psychological & Brain Sciences, Dartmouth College, Hanover, NH, 03755

17 <sup>5</sup>Center for Neural Science, New York University, New York, NY, 10003

18 <sup>6</sup>Neuroscience Institute at the NYU Langone Medical Center, New York, NY, 10016

19

20

21 *\*Correspondence:*

22 Denise J. Cai

23 Nash Department of Neuroscience, Icahn School of Medicine at Mount Sinai

24 One Gustave L. Levy Place

25 Box 1639

26 New York, NY 10029

27 Email: denisecai@gmail.com

28

29

30

31 **Keywords**

32 hippocampus, memory integration, memory-linking, ensemble, reactivation, co-firing, offline periods,  
33 stress, PTSD

## 34 **Abstract**

35           Memories are encoded in neural ensembles during learning and stabilized by post-learning  
36 reactivation. Integrating recent experiences into existing memories ensures that memories contain the  
37 most recently available information, but how the brain accomplishes this critical process remains  
38 unknown. Here we show that in mice, a strong aversive experience drives the offline ensemble  
39 reactivation of not only the recent aversive memory but also a neutral memory formed two days prior,  
40 linking the fear from the recent aversive memory to the previous neutral memory. We find that fear  
41 specifically links retrospectively, but not prospectively, to neutral memories across days. Consistent  
42 with prior studies, we find reactivation of the recent aversive memory ensemble during the offline period  
43 following learning. However, a strong aversive experience also increases co-reactivation of the aversive  
44 and neutral memory ensembles during the offline period. Finally, the expression of fear in the neutral  
45 context is associated with reactivation of the shared ensemble between the aversive and neutral  
46 memories. Taken together, these results demonstrate that strong aversive experience can drive  
47 retrospective memory-linking through the offline co-reactivation of recent memory ensembles with  
48 memory ensembles formed days prior, providing a neural mechanism by which memories can be  
49 integrated across days.

50

## 51 **Main Text**

52           Individual memories are initially encoded by ensembles of cells active during a learning event<sup>1-5</sup>  
53 and are stabilized during offline periods following learning through reactivation of those ensembles<sup>6-17</sup>.  
54 These reactivations often occur in brief synchronous bursts, which are necessary to drive memory  
55 consolidation<sup>18-20</sup>. Most research on episodic memory has focused on how the brain maintains stable  
56 representations of discrete memories; however, animals are constantly aggregating new memories and  
57 updating past memories as new, relevant information is learned<sup>21</sup>. Moreover, most studies of  
58 associative learning have focused on cues that directly precede or occur with an outcome. However,  
59 oftentimes in nature, a predictor may not immediately precede an outcome but animals are nonetheless  
60 capable of learning to make an inference about the association (e.g., conditioned taste aversion)<sup>22</sup>. It is  
61 unclear the environmental variables that could promote memories to be linked across long periods (i.e.,

62 days), and the neural mechanisms of memory integration across such disparate time periods are poorly  
63 understood. In addition, while it has been shown that offline periods support memory consolidation,  
64 recent studies have suggested that offline periods following learning may be important for memory  
65 integration processes as well<sup>23-26</sup>.

66

### 67 **Strong aversive experience drives retrospective memory-linking**

68 To investigate how memories are integrated across days, we first designed a behavioral  
69 experiment to test whether mice would spread fear from an aversive memory to a neutral memory  
70 formed two days prior (Retrospective memory-linking) or two days after (Prospective memory-linking)  
71 (Figure 1A). In the Retrospective group, mice first experienced a Neutral context followed by an  
72 Aversive context paired with a foot shock two days later. In the Prospective group, mice experienced an  
73 Aversive context followed by a Neutral context two days later. Both groups were then tested in the  
74 Aversive context to test for recall of the aversive memory, followed by testing in the previously  
75 experienced Neutral context or an unfamiliar Novel context to test for non-specific fear generalization.  
76 Memory-linking was defined as a selective increase in fear in the Neutral context compared to the  
77 Novel context, both contexts in which they had never been shocked. Notably, this definition  
78 distinguishes memory-linking from a broader generalization of fear across contexts. Mice froze no  
79 differently in the Aversive context in either group, suggesting that the perceived negative valence of the  
80 Aversive context was not different between groups (Figure 1B). Interestingly, in the Retrospective  
81 group, mice froze more in the Neutral context compared to the Novel context, suggesting that fear  
82 spread retrospectively from the Aversive context to the Neutral context experienced two days prior.  
83 However, in the Prospective group, there was no difference in freezing between the Neutral and Novel  
84 contexts, suggesting that memory-linking between the Aversive and Neutral contexts did not occur  
85 prospectively across days (Figure 1C). Consistent with prior studies, mice froze in the Neutral context in  
86 both Prospective and Retrospective conditions when the Neutral and Aversive contexts were  
87 experienced within a day (5h apart, Extended Figure 1A)<sup>27,28</sup>. However, when the contexts were  
88 separated by more than one day, mice froze in the Neutral context only in the Retrospective and not the  
89 Prospective condition (Extended Figure 1B).

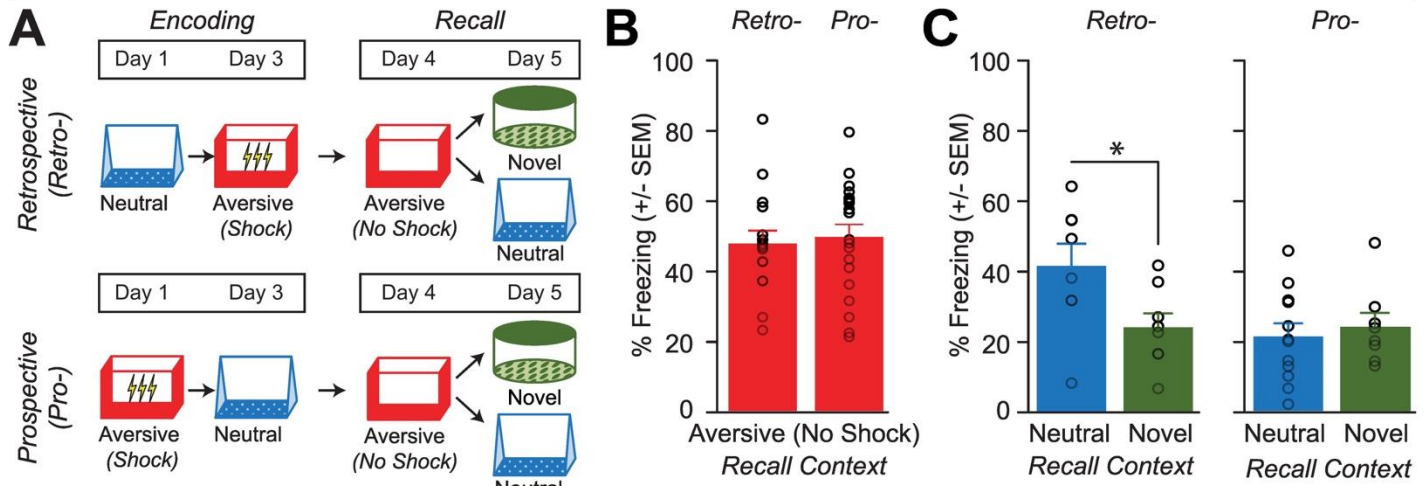
90 We next asked what environmental variables drove two memories to be linked retrospectively  
91 across days. It has previously been suggested that the emotional salience of an experience enhances  
92 its storage into memory<sup>29,30</sup>, as well as its likelihood of altering past neutral memories in humans<sup>31</sup>.  
93 Thus, we hypothesized that the more aversive the experience, the more likely that fear would be  
94 retrospectively linked to a previous neutral memory. To test this, we manipulated the shock intensity  
95 during aversive encoding to test if stronger shock would drive retrospective memory-linking (Figure 1D).  
96 Mice were exposed to a Neutral context followed by an Aversive context paired with a low or high shock  
97 two days later (Low Shock group & High Shock group). Mice were then tested in the Aversive, Neutral,  
98 and a Novel context in the subsequent three days. As expected, mice in the High Shock group froze  
99 more than mice in the Low Shock group during recall in the Aversive context (Figure 1E). We found that  
100 only High Shock mice exhibited a selective increase in freezing in the previously experienced Neutral  
101 context relative to the Novel context during recall (Figure 1F; Extended Figure 1C-E). If the perceived  
102 aversiveness of an experience affects the likelihood of retrospective memory-linking, we hypothesized  
103 that levels of freezing during Aversive memory recall would positively correlate with memory-linking—  
104 defined as the difference between freezing in the Neutral context and in the Novel context. Indeed, in  
105 the High Shock mice, the freezing during Aversive context recall positively correlated with the degree of  
106 memory-linking (Figure 1G).

107 We next investigated how the brain links recent aversive memories with past neutral memories  
108 formed days prior. It has been well established in rodents and humans that memories are reactivated  
109 during restful periods following learning (i.e., offline periods) to promote the storage of recently learned  
110 information<sup>17,32-34</sup>. However, recent work in humans has shown that offline periods can drive the  
111 integration of discrete memories as well<sup>23,35,36</sup>. Thus, we hypothesized that following an aversive  
112 experience (High Shock group), the offline period may be serving not only to support the consolidation  
113 of the aversive memory, but also to link the recent aversive memory with the prior neutral memory, thus  
114 increasing freezing during recall of the Neutral context. A major site of memory formation in the brain is  
115 the hippocampus, where rapid plasticity following an experience promotes the formation of a memory  
116 for that experience and reflects memory expression thereafter<sup>18,27,37-39</sup>. Thus, we asked whether  
117 hippocampal activity during the offline period following Aversive encoding was necessary to drive

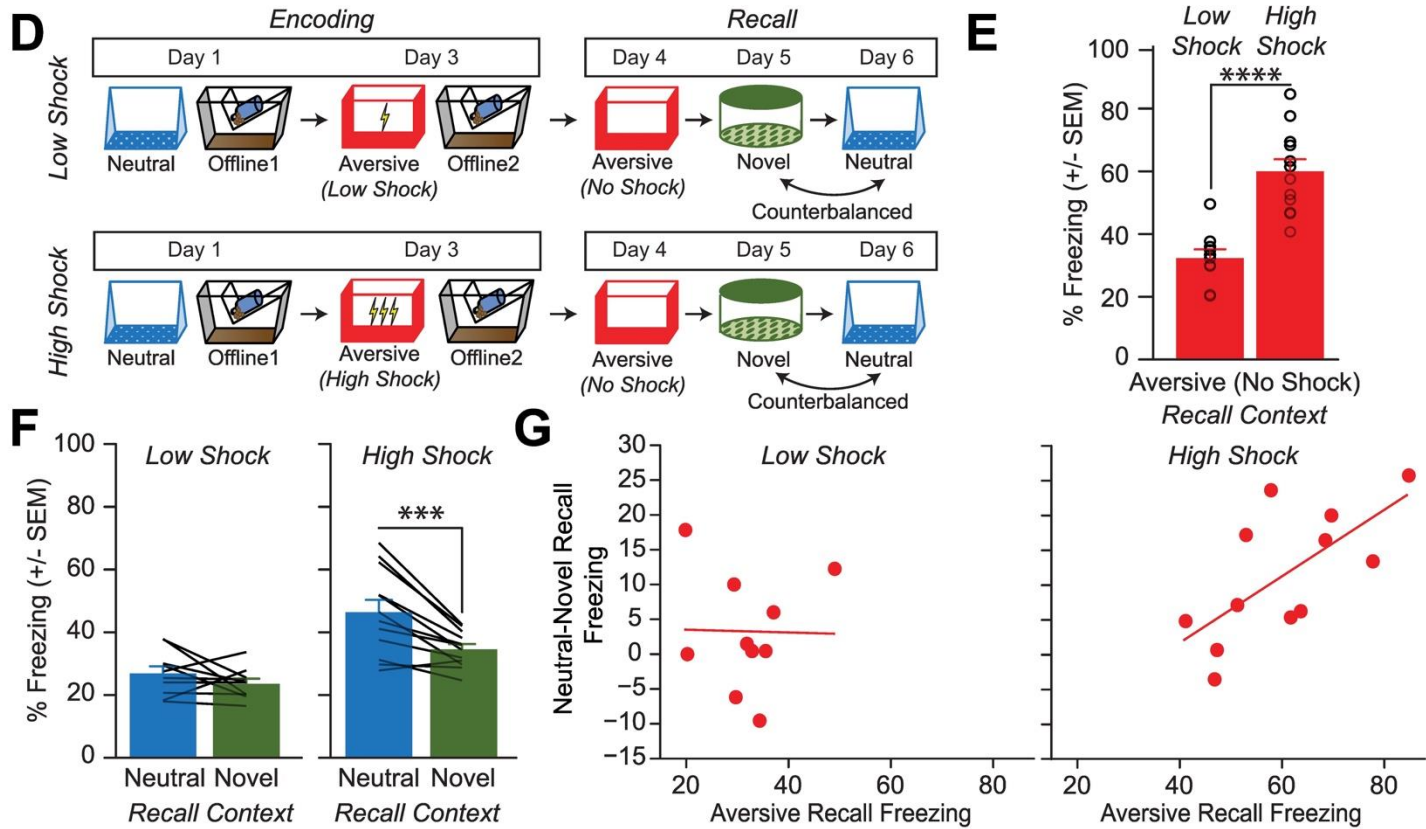
118 retrospective memory-linking. To do this, we used a chemogenetic manipulation system to disrupt  
119 endogenous hippocampal activity during the offline period following Aversive encoding paired with a  
120 strong shock (Extended Figure 2). We predicted that this would disrupt retrospective memory-linking.  
121 Prior studies have shown that PSAM4-GlyR (PSAM) is an inhibitory ionotropic receptor with no  
122 endogenous ligand, and binding of the PSEM ligand with the PSAM receptor causes robust  
123 hyperpolarization in neurons<sup>40</sup>. We injected mice with a pan-neuronal, PSAM4-GlyR-expressing virus  
124 bilaterally in hippocampus and during the offline period immediately following Aversive encoding, we  
125 administered either PSEM to manipulate offline hippocampal activity, or injected saline as a control. We  
126 found that mice that received saline during the offline period exhibited a selective increase in freezing in  
127 the Neutral over the Novel context, demonstrating retrospective memory-linking. In contrast, mice that  
128 received PSEM no longer showed this selective increase in freezing in the Neutral context (Extended  
129 Figure 2A-C). To ensure that this effect on retrospective memory-linking was not due to a disrupted  
130 memory for the Aversive context, we repeated the experiment, administering PSEM or saline during the  
131 offline period, and then tested mice in the Aversive context. We found that mice that received PSEM  
132 froze no differently compared to saline controls during Aversive memory recall, suggesting that the  
133 strong aversive memory was left intact (Extended Figure 2D,E). These results suggest that  
134 hippocampal activity during the offline period is necessary to drive retrospective memory-linking.

135 **Figure 1**

**Prospective vs. Retrospective Memory-Linking**



**Low Shock vs. High Shock Retrospective Memory-Linking**



136 **Figure 1. Strong aversive experience drives retrospective memory-linking to a neutral context learned**  
137 **days ago.** A) Schematic of prospective vs retrospective memory-linking behavior experiment. Mice either  
138 received a Neutral experience followed by an Aversive experience two days later (Retrospective) or the Aversive  
139 experience followed by Neutral (Prospective). One day after the second experience, mice were tested in the  
140 Aversive context they were shocked in. The following day, mice were tested in either the previously experienced  
141 Neutral context or a Novel context.  
142  
143 B) Freezing during Aversive recall in Prospective vs Retrospective groups. There was no difference in Aversive  
144 recall freezing between Prospective & Retrospective conditions ( $t_{34} = 0.36$ ,  $p = 0.72$ ) (*Retrospective*,  $N = 16$  mice;  
145 *Prospective*,  $N = 20$  mice).  
146  
147 C) Freezing during Neutral vs Novel recall in Prospective vs Retrospective groups. There was a significant  
148 interaction between freezing in Neutral vs Novel recall in the Retrospective vs Prospective groups, suggesting the  
149 Aversive experience retrospectively linked to the Neutral memory, but not prospectively. Significant interaction  
150 between Direction (Prospective vs Retrospective) and Context (Neutral vs Novel), ( $F_{1,32} = 4.90$ ,  $p = 0.034$ )  
151 (*Retrospective Neutral*,  $N = 8$  mice; *Retrospective Novel*,  $N = 8$  mice; *Prospective Neutral*,  $N = 12$  mice,  
152 *Prospective Novel*,  $N = 8$  mice). Post-hoc, *Retrospective* ( $t_{32} = 2.586$ ,  $p = 0.029$ ), *Prospective* ( $t_{32} = 0.452$ ,  $p =$   
153  $0.6546$ ).  
154  
155 D) Schematic of Low Shock vs High Shock retrospective memory-linking experiment. Mice received a Neutral  
156 experience followed by a 1hr offline session in their homecage. Two days later, they received either 3 low shocks  
157 (0.25mA) or 3 high shocks (1.5mA, same amplitude as in Figure 1A) in an Aversive context, followed by another  
158 1hr offline session in their homecage. The following day they were tested in the Aversive context, and for the  
159 following two days they were tested in the Neutral and Novel contexts, counterbalanced. Calcium imaging was  
160 performed during all the sessions.  
161  
162 E) Freezing during Aversive recall in Low vs High Shock mice. Mice froze more in the Aversive context after  
163 receiving a high shock vs low shock ( $t_{18,8} = 5.877$ ,  $p = 0.000012$ ) (*Low Shock*,  $N = 10$  mice; *High Shock*,  $N = 12$   
164 *mice*).  
165  
166 F) Freezing during Neutral vs Novel recall in Low vs High Shock mice. Mice only displayed enhanced freezing in  
167 Neutral vs Novel (i.e., retrospective memory-linking) after High Shock and not Low Shock. Significant effect of  
168 Context (Neutral vs Novel) ( $F_{1,20} = 17.32$ ,  $p = 0.000048$ ) and significant interaction between Context and  
169 Amplitude ( $F_{1,20} = 4.99$ ,  $p = 0.037$ ) (*Low Shock*,  $N = 10$  mice; *High Shock*,  $N = 12$  mice). High Shock mice froze  
170 more in the Neutral vs Novel contexts ( $t_{11} = 4.37$ ,  $p = 0.002$ ) while Low Shock mice froze no differently in the two  
171 contexts ( $t_9 = 1.23$ ,  $p = 0.249$ ).  
172  
173 G) Correlation between Aversive recall freezing and memory-linking strength. The strength of the aversive  
174 memory was correlated with the degree of retrospective memory-linking in High Shock mice ( $R^2 = 0.45$ ,  $p =$   
175  $0.016$ ), but not in Low Shock mice ( $R^2 = 0.0003$ ,  $p = 0.963$ ) (*Low Shock*,  $N = 10$  mice; *High Shock*,  $N = 12$  mice).

## 176 **Strong aversive learning drives offline reactivation of a past neutral ensemble**

177 Previous work has suggested that memory reactivation during offline periods following learning  
178 could promote not only the consolidation of recently formed memories, but also support the integration  
179 of memories<sup>23,25,26,35,36,41</sup>. Consistent with previous studies, we expected that during the offline period  
180 following Aversive encoding (while mice are in their homecage), the ensemble active during Aversive  
181 encoding would be reactivated to drive consolidation of the recently learned aversive memory.  
182 However, we also hypothesized that if the aversive experience was strong enough, the ensemble active  
183 during the neutral experience (from two days prior) would be reactivated as well, integrating the neutral  
184 and aversive memories.

185 We first validated that we could detect ensemble reactivation after a salient experience using  
186 calcium imaging. To do this, we conducted a contextual fear conditioning experiment, recording  
187 hippocampal CA1 calcium dynamics using the open-source UCLA Miniscopes<sup>27</sup> (Extended Figure  
188 3A,B). We recorded during Aversive encoding, the first hour offline following Aversive encoding, and  
189 during recall of the Aversive context and exposure to a Novel context. Consistent with previous  
190 literature, we found that the ensemble of cells active during Aversive encoding was reactivated offline  
191 and preferentially reactivated during Aversive memory recall, suggesting a stable neural memory  
192 ensemble (Extended Figure 3C-K).

193 To next investigate whether a strong aversive experience was driving offline reactivation of  
194 ensembles representing both the aversive and neutral memories, we performed calcium imaging  
195 recordings in CA1 during the offline periods following the initial Neutral experience (Offline1) and  
196 subsequent Aversive experience (Offline2) in both Low and High Shock groups (Figure 2; Extended  
197 Figure 4; same experiment as in Figure 1D). Consistent with the literature<sup>18,20</sup> and with our previous  
198 experiment (Extended Figure 3), following the initial Neutral encoding, the cells that were active during  
199 that experience (Neutral ensemble) were more active compared with cells not active during Neutral  
200 encoding (Remaining ensemble) in both Low and High Shock groups (Figure 2B, line graphs). There  
201 was no difference in the fraction of cells that made up the Neutral ensemble in the Low vs High Shock  
202 groups (Figure 2B, pie charts). To measure ensemble reactivation during the offline period after  
203 Aversive encoding, we separated cells that were active during the offline period into four ensembles



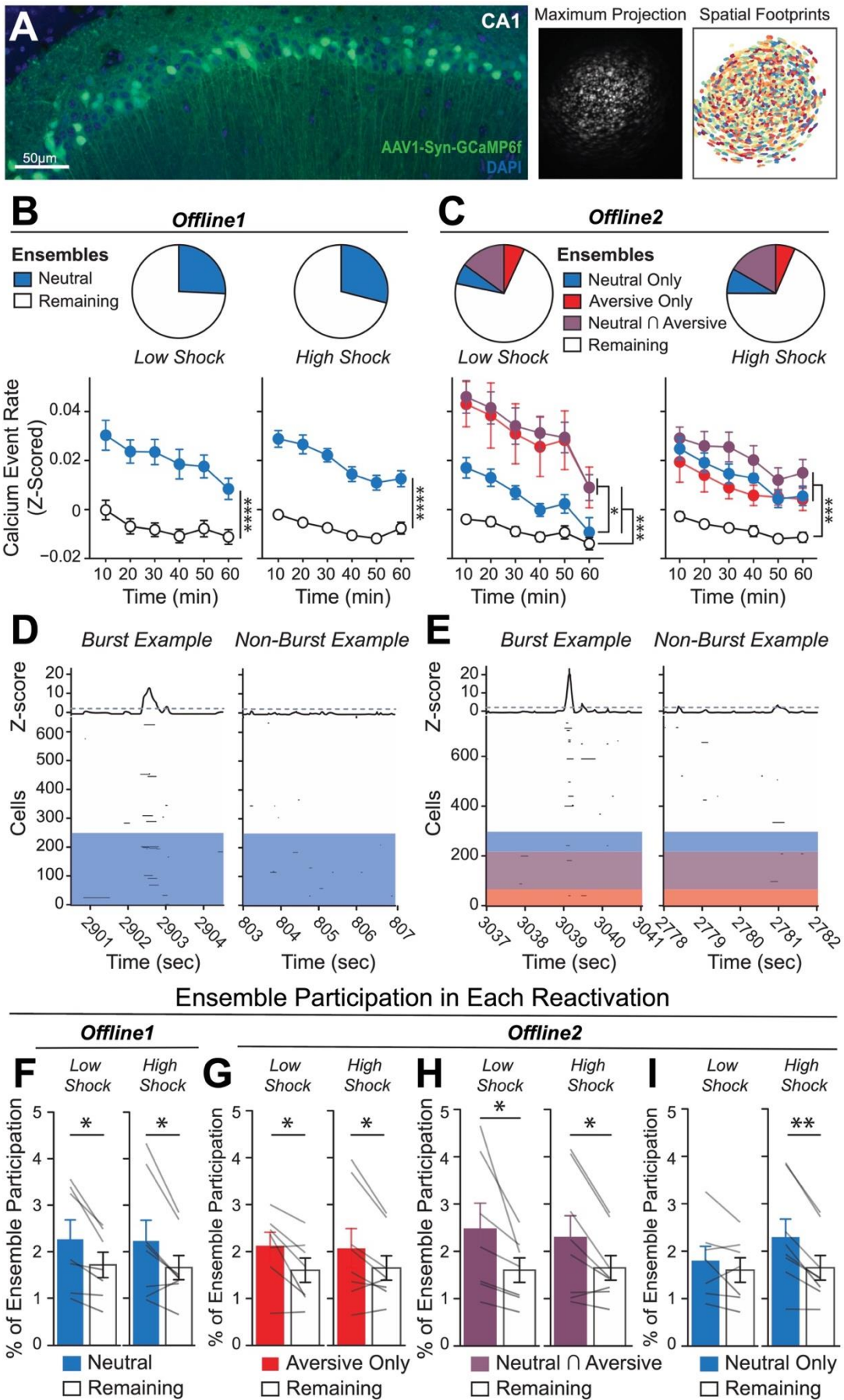
204 based on when those cells were previously active: Neutral ensemble represented cells active during the  
205 initial Neutral encoding and not Aversive encoding; Aversive ensemble represented cells active during  
206 Aversive encoding and not Neutral encoding; Neutral  $\cap$  Aversive ensemble represented cells that were  
207 active during both Neutral and Aversive encoding; and Remaining ensemble represented cells not  
208 observed to be active prior to the offline period (Figure 2C). There was no difference in the fraction of  
209 cells that made up each ensemble across Low and High Shock groups (Figure 2C, pie charts). In the  
210 Low Shock group, consistent with prior literature<sup>14</sup>, we found the Aversive ensemble, the Neutral  
211 ensemble, and the Neutral  $\cap$  Aversive ensemble had higher calcium activity than the Remaining  
212 ensemble. And the Neutral ensemble was less active than the Aversive and Neutral  $\cap$  Aversive  
213 ensembles (Figure 2C, line graphs, left side). These results are consistent with prior studies  
214 demonstrating offline reactivation of neuronal ensembles that were recently active during learning<sup>7-9</sup>. In  
215 contrast, in the High Shock group, the Neutral ensemble was no differently active than the Aversive and  
216 Neutral  $\cap$  Aversive ensembles (Figure 2C, line graphs, right side), indicating that the high shock  
217 increased reactivation of the Neutral ensemble.

218         Since the Neutral ensemble was more highly reactivated after high shock, we next investigated  
219 whether the Neutral, Aversive, and Neutral  $\cap$  Aversive ensembles might be firing together on a finer  
220 temporal scale. Hippocampal activity is known to exhibit organized bursts, oftentimes accompanied by  
221 sharp-wave ripples in the local field potential, during which cells active during learning are preferentially  
222 reactivated<sup>18</sup>. These events have been found to support memory consolidation<sup>18-20</sup>. Although calcium  
223 dynamics are of a coarser timescale than sharp-wave ripples, we observed that during the offline  
224 recordings, hippocampal calcium activity periodically exhibited brief bursts of activity during which  
225 numerous cells were co-active (Extended Figure 5A,B, from our validation study in Extended Figure 3),  
226 consistent with previous reports<sup>42,43</sup>. We found that these bursts were unlikely to occur from shuffled  
227 neuronal activities, suggesting that these events were organized events during which groups of  
228 hippocampal neurons were synchronously active (Extended Figure 5C-F). We isolated these brief burst  
229 periods to ask whether ensembles that were previously active during encoding were selectively  
230 participating in these brief burst events (Figure 2D-I; Extended Figure 5A,B; see Methods). We first  
231 measured these burst events after a single Aversive learning experience and found that a larger

232 fraction of Aversive ensemble cells participated in these events than the Remaining ensemble cells  
233 (Extended Figure 5L). Interestingly, these burst events coincided with the mouse briefly slowing down  
234 about 1 second prior to the event, and about 1 second after its onset resuming its locomotion,  
235 suggesting that these bursts occurred during periods of brief quiescence (Extended Figure 5I,J)<sup>18</sup>.

236 We then asked whether a strong shock paired with an Aversive context would drive the Neutral  
237 ensemble to also participate within these bursts after Aversive encoding (experiment from Figure 1D).  
238 In both Low and High Shock mice and after both Neutral and Aversive encoding, frequencies of burst  
239 events (defined by periods when the mean activity of the entire recorded population reached above a  
240 required threshold; see Methods) were comparable across groups and decreased across the hour  
241 (Extended Figure 4G,H). As expected, after Neutral encoding, both Low and High Shock groups had a  
242 larger fraction of the Neutral ensemble participating in these burst events than the Remaining ensemble  
243 (Figure 2D,F). After Aversive encoding, both groups again showed selective participation of the  
244 Aversive ensemble that was most recently active (Figure 2G) as well as of the Neutral  $\cap$  Aversive  
245 ensemble that was previously active during both learning events (Figure 2H). However, only in the High  
246 Shock group (and not the Low Shock group) the Neutral ensemble selectively participated in these  
247 burst events as well (Figure 2I), suggesting that a strong aversive experience drove the recruitment of  
248 the Neutral ensemble into these burst events.

249 **Figure 2**



250 **Figure 2. Strong aversive experience drives reactivation of a past neutral ensemble.**

- 251  
252 A) Representative histology (left) of GCaMP6f expression in hippocampal CA1, imaged with a confocal  
253 microscope. Green represents AAV1-Syn-GCaMP6f expression, while blue represents a cellular DAPI stain.  
254 Maximum intensity projection of an example mouse across one recording session, imaged with a Miniscope  
255 (middle), with the spatial footprints of all recorded cells during that session (right) randomly color-coded.  
256
- 257 B) During Offline1 after Neutral encoding, cells that were active during Neutral encoding (Neutral ensemble) made  
258 up ~25-30% of the offline cell population (pie charts) ( $\chi^2 = 0.122$ ,  $df = 1$ ,  $p = 0.73$ ). The Neutral ensemble was  
259 more highly active than the Remaining ensemble during the offline period (line graphs; A.U.). There was a main  
260 effect of Ensemble ( $F_{1,159} = 59.19$ ,  $p = 1.4e-12$ ), no effect of Amplitude ( $F_{1,13} = 0.039$ ,  $p = 0.85$ ), and an effect of  
261 Time ( $F_{1,159} = 4.33$ ,  $p = 0.039$ ), and all interactions  $p > 0.05$  (Low Shock,  $N = 7$  mice; High Shock,  $N = 8$  mice).  
262
- 263 C) During Offline2 after Aversive encoding, similar proportions of previously active cells were reactivated across  
264 Low and High shock groups (pie charts) ( $\chi^2 = 0.326$ ,  $df = 3$ ,  $p = 0.955$ ). However, ensembles were differentially  
265 reactivated based upon the amplitude of the Aversive experience (Ensemble  $\times$  Amplitude:  $F_{3,331} = 5.36$ ,  $p =$   
266  $0.0013$ ) (line graphs; A.U.). In Low Shock mice, the Neutral, Aversive, and Neutral  $\cap$  Aversive ensembles were  
267 more highly active than the Remaining ensemble (contrast,  $t_{18} = 4.22$ ,  $p = 0.0005$ ). Additionally, these ensembles  
268 were differentially active relative to one another ( $F_{2,12} = 4.03$ ,  $p = 0.046$ ). This was driven by the Neutral ensemble  
269 being less active. The Neutral ensemble was less active than the Aversive and Neutral  $\cap$  Aversive ensembles ( $t_{12}$   
270  $= 2.83$ ,  $p = 0.03$ ) while the Aversive ensemble was no differently active than the Neutral  $\cap$  Aversive ensemble ( $t_{12}$   
271  $= 0.19$ ,  $p = 0.85$ ). In High Shock mice, the Neutral, Aversive, and Neutral  $\cap$  Aversive ensembles were all more  
272 highly active than the Remaining ensemble ( $t_{21} = 4.36$ ,  $p = 0.0003$ ), but these three ensembles were no differently  
273 active from each other ( $F_{2,14} = 1.52$ ,  $p = 0.25$ ) (Low Shock,  $N = 7$  mice; High Shock,  $N = 8$  mice).  
274
- 275 D) During the offline periods, hippocampal activity displayed brief bursts of neural activity. To detect these bursts,  
276 we computed the z-scored mean activity of the entire recorded population and applied a threshold of  $z=2$  and  
277 defined burst periods as all the timepoints above this threshold. The left raster represents an example burst  
278 period during Offline1, during which mean population activity briefly reached above threshold. Each row of the  
279 raster represents the activity of every recorded neuron, color-coded based on the ensemble it was a part of (blue  
280 represents Neutral ensemble and grey represents Remaining ensemble; see legend in Figure 2B). The top black  
281 trace represents the z-scored mean population activity. The right raster represents an example non-burst period.  
282
- 283 E) Same as D but an example burst and non-burst period for Offline2. Each row of the raster again is color-coded  
284 based on the ensemble it was a part of (Aversive in red, Neutral  $\cap$  Aversive in purple, Neutral in blue, and  
285 Remaining in grey; see legend in Figure 2C).  
286
- 287 F) During Offline1 in both Low and High Shock groups, a larger fraction of the Neutral ensemble participated in  
288 bursts than the Remaining ensemble did (Ensemble:  $F_{1,13} = 16.33$ ,  $p = 0.001$ ; Amplitude:  $F_{1,13} = 0.009$ ,  $p =$   
289  $0.925$ ; Ensemble  $\times$  Amplitude:  $F_{1,13} = 0.0058$ ,  $p = 0.940$ ) (Low Shock,  $N = 7$  mice; High Shock,  $N = 8$  mice).  
290
- 291 G) During Offline2 in both Low and High Shock groups, a larger fraction of the Aversive ensemble participated in  
292 bursts than the Remaining ensemble (Ensemble:  $F_{1,13} = 13.57$ ,  $p = 0.0028$ ; Amplitude:  $F_{1,13} = 0.000078$ ,  $p = 0.99$ ;  
293 Ensemble  $\times$  Amplitude:  $F_{1,13} = 0.16$ ,  $p = 0.69$ ) (Low Shock,  $N = 7$  mice; High Shock,  $N = 8$  mice).  
294
- 295 H) During Offline2 in both Low and High Shock groups, a larger fraction of the Neutral  $\cap$  Aversive ensemble  
296 participated in bursts than the Remaining ensemble (Ensemble:  $F_{1,13} = 13.95$ ,  $p = 0.0025$ ; Amplitude:  $F_{1,13} =$   
297  $0.014$ ,  $p = 0.91$ ; Ensemble  $\times$  Amplitude:  $F_{1,13} = 0.31$ ,  $p = 0.58$ ) (Low Shock,  $N = 7$  mice; High Shock,  $N = 8$  mice).  
298
- 299 I) During Offline2, Neutral and Remaining ensembles differentially participated in bursts in High and Low Shock  
300 groups (Ensemble  $\times$  Amplitude:  $F_{1,13} = 5.186$ ,  $p = 0.040$ ). High Shock mice showed higher participation of the  
301 Neutral ensemble relative to Remaining ensemble ( $t_7 = 4.88$ ,  $p = 0.0036$ ), whereas Low Shock mice showed no  
302 different participation between the two ensembles ( $t_6 = 1.33$ ,  $p = 0.23$ ) (Low Shock,  $N = 7$  mice; High Shock,  $N = 8$   
303 mice).

304 **Strong aversive experience drives co-bursting of the Neutral  $\cap$  Aversive ensemble with the**  
305 **Neutral ensemble**

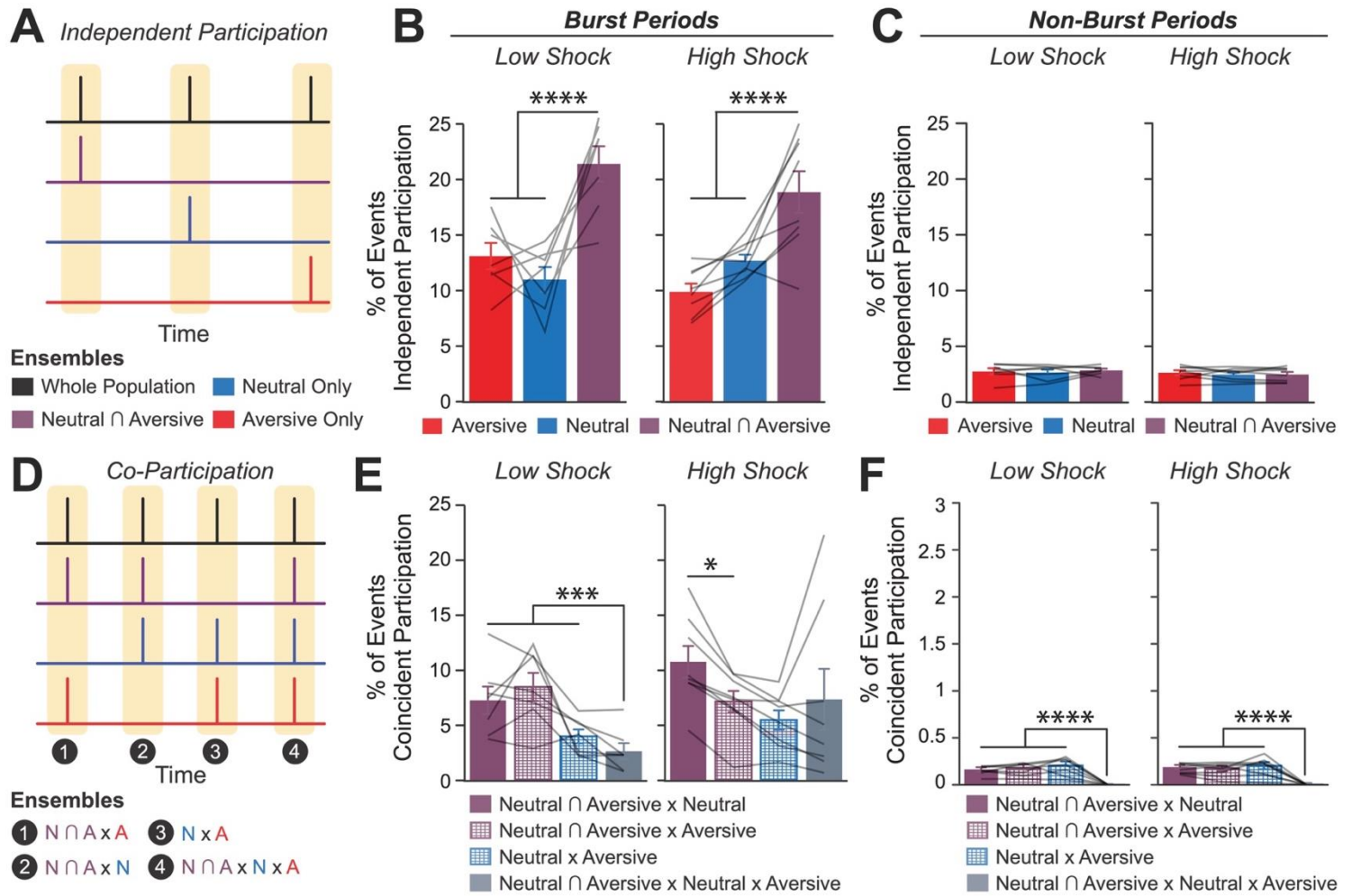
306 Since after High Shock, the Neutral and Aversive ensembles were both participating in burst  
307 events, we next asked whether the two ensembles co-participated within the same bursts, or whether  
308 they participated separately in different bursts. Co-bursting between the Neutral ensemble and Aversive  
309 ensemble could suggest a process through which the two ensembles can become integrated into a cell  
310 assembly likely to co-fire during memory recall thereafter. This process could occur through Hebbian  
311 plasticity<sup>44</sup> or through behavioral timescale synaptic plasticity, which has been proposed to drive the  
312 formation of place fields in hippocampal neurons<sup>37</sup>. Previous work has shown that hippocampal  
313 neurons become highly co-active during recall of an aversive memory but not during initial learning<sup>45</sup>,  
314 that co-activity relationships among hippocampal neurons can distinguish between contexts that a  
315 mouse has experienced<sup>46</sup>, and that ensembles that are highly co-active during an offline period  
316 following learning are more likely to be reactivated during memory recall than non-co-active neurons<sup>15</sup>.

317 To ask whether the Neutral, Aversive, and Neutral  $\cap$  Aversive ensembles were co-bursting after  
318 Aversive encoding, we measured the fraction of burst events that each ensemble participated in  
319 independently of each other (Figure 3A) and the fraction that the ensembles co-participated in (Figure  
320 3D) during the offline period following the Aversive experience (Extended Figure 4I; see Methods).  
321 Previously, we had found that the Neutral  $\cap$  Aversive cells (those active during both Neutral and  
322 Aversive encoding) were the most highly active during the offline period (Figure 2C). Highly active  
323 subpopulations of neurons have been proposed to form a 'hub-like' population of neurons that may  
324 orchestrate the activity of other neurons in a larger network<sup>47,48</sup>. Therefore, these highly active neurons  
325 could be organizing the activity of other neurons in the hippocampus to drive activity during this offline  
326 period. Thus, we hypothesized that co-participation between the highly active Neutral  $\cap$  Aversive  
327 ensemble and the Neutral ensemble would be enhanced after a strong aversive experience.

328 We found that during burst events, the Neutral  $\cap$  Aversive ensemble participated independently  
329 more frequently than the Neutral and Aversive ensembles did, but there was no difference between  
330 Low and High Shock mice (Figure 3B). Notably, during non-burst periods, independent ensemble  
331 bursting did not vary between any of the ensembles (Figure 3C). We next measured co-participation of

332 the ensembles in all combinations (Figure 3D). We found that in the Low Shock group, co-participation  
333 between the three ensembles was less likely to occur than the other combinations; however,  
334 surprisingly, in the High Shock group, co-participation between the three ensembles was no different  
335 from the other combinations (Figure 3E). Additionally, in the High Shock group, the Neutral  $\cap$  Aversive  
336 ensemble co-participated with the Neutral ensemble more than it did with the Aversive ensemble,  
337 whereas in the Low Shock group, the Neutral  $\cap$  Aversive ensemble co-participated no differently with  
338 the Neutral and Aversive ensembles (Figure 3E). Importantly, there were no differences in ensemble  
339 co-bursting between Low and High Shock groups during non-burst periods (Figure 3F), suggesting that  
340 the ensemble co-participation was confined to periods when the hippocampus was synchronously  
341 active. These results suggested that after a strong aversive experience, the Neutral  $\cap$  Aversive  
342 ensemble was preferentially co-bursting with the Neutral ensemble. To confirm that this was the case,  
343 we used cross-correlations as another measure of co-activity to measure how co-active the Neutral  $\cap$   
344 Aversive ensemble was with the Neutral and the Aversive ensembles. Indeed, only in the High Shock  
345 group, the Neutral  $\cap$  Aversive ensemble was preferentially correlated with the Neutral ensemble  
346 compared with the Aversive ensemble during the offline period (Extended Figure 4K). Collectively,  
347 these results suggest that a strong aversive experience increases the co-bursting of the Neutral  $\cap$   
348 Aversive ensemble with the Neutral ensemble, perhaps to link fear of the recent aversive experience  
349 with the past neutral memory.

350 **Figure 3**



351 **Figure 3. Strong aversive experience drives co-reactivation of the Neutral ensemble with the Neutral  $\cap$**   
352 **Aversive ensemble.**

- 353  
354 A) Representation of the quantification of independent participation during bursts versus non-bursting periods.  
355 Burst events were defined by the whole recorded population, as in Figure 2E (outlined by yellow rectangles).  
356 However, now the z-scored mean population activity of the Aversive, Neutral, and Neutral  $\cap$  Aversive ensembles  
357 was computed to ask how frequently each ensemble participated in whole population bursts independently of one  
358 another. Independent participation meant one ensemble participated while the other two did not.  
359  
360 B) During burst periods, the Neutral  $\cap$  Aversive ensemble participated independently in more bursts than the  
361 Aversive ensemble ( $t_{14} = 7.95$ ,  $p = 0.000002$ ) and more than the Neutral ensemble ( $t_{14} = 5.59$ ,  $p = 0.0001$ ) but  
362 there was no difference in participation across Low vs High Shock mice ( $F_{1,13} = 1.43$ ,  $p = 0.25$ ) and no interaction  
363 ( $F_{2,26} = 2.49$ ,  $p = 0.10$ ) (Low Shock,  $N = 7$  mice; High Shock,  $N = 8$  mice).  
364  
365 C) During non-burst periods, there was no difference in participation across ensembles ( $F_{2,26} = 0.38$ ,  $p = 0.69$ ) or  
366 between Low and High Shock mice ( $F_{1,13} = 0.73$ ,  $p = 0.41$ ), and no interaction ( $F_{2,26} = 0.36$ ,  $p = 0.70$ ) (Low Shock,  
367  $N = 7$  mice; High Shock,  $N = 8$  mice).  
368  
369 D) Representation of the quantification of co-participation during bursts vs non-bursting periods. As in Figure 3B,  
370 the whole population was used to define bursts and the z-scored mean population activities were used to define  
371 participation of each ensemble. Co-participation was defined as a whole population burst (outlined by yellow  
372 rectangles) during which multiple ensembles participated simultaneously. There were four possible combinations  
373 (from left to right: N $\cap$ A x N, N $\cap$ A x A, N x A, N $\cap$ A x N x A) (N $\cap$ A = Neutral  $\cap$  Aversive; N = Neutral; A = Aversive).  
374  
375 E) During burst periods, there was a significant interaction between Ensemble Combination and Low vs High  
376 Shock ( $p = 0.01$ ), suggesting that the patterns of co-bursting varied in Low vs High Shock mice. Post-hoc tests  
377 revealed that in Low Shock mice, co-participation between all 3 ensembles was less likely to occur than the other  
378 combinations ( $t_{18} = 4.73$ ,  $p = 0.0003$ ), while in High Shock mice, co-participation between all 3 ensembles  
379 occurred no differently than the other combinations ( $t_{21} = 0.358$ ,  $p = 0.72$ ). Additionally, in the High Shock group,  
380 the N $\cap$ A ensemble preferentially co-participated with the Neutral ensemble compared to with the Aversive  
381 ensemble ( $t_{21} = 2.373$ ,  $p = 0.05$ ), whereas in the Low Shock group, the N $\cap$ A ensemble participated no differently  
382 with the Neutral and Aversive ensembles ( $t_{18} = 1.196$ ,  $p = 0.25$ ) (Low Shock,  $N = 7$  mice; High Shock,  $N = 8$   
383 mice).  
384  
385 F) During non-burst periods, co-participation between all 3 ensembles was less likely than the other combinations  
386 ( $t_{39} = 10.92$ ,  $p = 1.98e-13$ ); however, there was no effect of Low vs High Shock ( $F_{1,13} = 0.038$ ,  $p = 0.847$ ) and no  
387 interaction ( $F_{3,39} = 0.198$ ,  $p = 0.897$ ) (Low Shock,  $N = 7$  mice; High Shock,  $N = 8$  mice).



388 **Strong aversive experience drives co-reactivation of the Neutral & Aversive and Neutral**  
389 **ensembles during Neutral context recall**

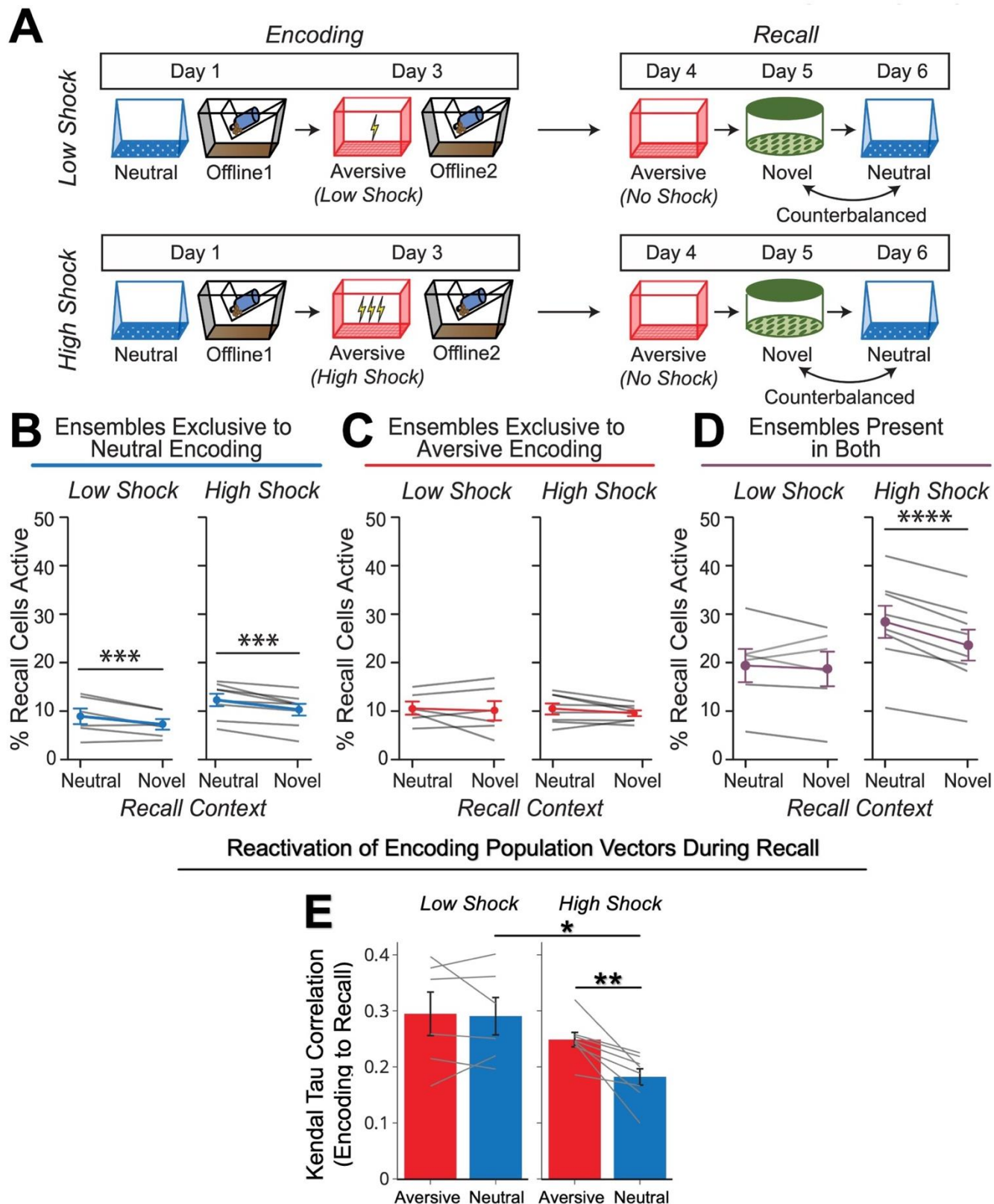
390 Finally, we asked whether hippocampal ensemble reactivation could support the freezing  
391 observed in the Neutral context during recall after a high shock and not low shock (as shown in Figure  
392 1F). To do this, we measured hippocampal ensemble activity while mice recalled the Neutral context  
393 after the offline period, compared with ensemble activity when they were placed in a Novel context as a  
394 control (Figure 4A). Since High Shock mice froze significantly more in the Neutral vs Novel contexts  
395 during recall (Figure 1F), we hypothesized that Neutral context recall would drive the aversive memory  
396 representation to be reactivated, whereas exposure to a Novel context would not provoke the  
397 reactivation of the aversive memory representation. Previously, we found that during the offline period,  
398 the Neutral  $\cap$  Aversive ensemble specifically co-reactivated with the Neutral ensemble (Figure 3E,  
399 Extended Figure 4K), perhaps forming an integrated ensemble of neurons that is more likely to fire  
400 together in the future. If this were the case, when High Shock mice recalled the Neutral context and  
401 reactivated the Neutral ensemble, we predicted they might also reactivate the Neutral  $\cap$  Aversive  
402 ensemble, perhaps through a process of pattern completion<sup>49</sup>, thereby driving freezing in the Neutral  
403 context. Importantly, we expected this not to occur in Low Shock mice, where Neutral and Neutral  $\cap$   
404 Aversive ensemble co-reactivation was not observed, or in High Shock mice during Novel context  
405 exposure, since fear did not selectively spread to the Novel context (Figure 1F).

406 During recall of the Neutral context and exposure to a Novel context, we measured the fraction  
407 of cells active during that session which were previously active during encoding of the Neutral or  
408 Aversive contexts or active during both Neutral and Aversive encoding (Figure 4A; Extended Figure  
409 4E,F). We previously observed that during the offline period, the Neutral ensemble co-fired with the  
410 Neutral  $\cap$  Aversive after high shock but not after low shock (Figure 3D,E; Extended Figure 3K),  
411 potentially forming an integrated ensemble that is more likely to fire together later. Thus, we  
412 hypothesized that after high shock, during Neutral context recall, the Neutral ensemble (representing  
413 the Neutral context) would be reactivated, and this would, in turn, trigger reactivation of the Neutral  $\cap$   
414 Aversive ensemble. As expected, cells exclusively active during Neutral encoding and not Aversive  
415 encoding were more likely to be reactivated during Neutral recall than during Novel context exposure in

416 both Low Shock and High Shock groups, suggesting a stable and selective neural population  
417 representing the neutral memory (Figure 4B). The cells exclusively active during Aversive encoding  
418 were not selectively reactivated during Neutral or Novel contexts in either group (Figure 4C).  
419 Interestingly, the cells active during both Neutral and Aversive encoding (Neutral  $\cap$  Aversive ensemble)  
420 were more reactivated during Neutral recall than during Novel context exposure in the High Shock but  
421 not the Low Shock group (Figure 4D). This suggests that after ensemble co-reactivation during the  
422 offline period following high shock, the Neutral ensemble and the Neutral  $\cap$  Aversive ensembles were  
423 more likely to reactivate together during Neutral recall.

424         The high shock aversive experience prompted an ensemble from days ago to be reactivated  
425 offline. During subsequent Neutral recall, mice exhibited increased freezing despite never having been  
426 shocked in that context. Therefore, the memory of the Neutral context had been modified to become  
427 perceived as negative in High Shock mice. If this offline reactivation of the Neutral ensemble was  
428 indeed modifying the neutral memory representation, we hypothesized that during Neutral recall, the  
429 activity patterns observed would be different from the activity patterns observed during Neutral  
430 encoding in the High Shock mice, compared to in Low Shock mice, and perhaps compared to the  
431 change observed from Aversive encoding to Aversive recall. To test this, we computed a mean  
432 population activity vector during Neutral encoding and correlated it with 30-second population vectors  
433 across Neutral recall, to measure the similarity between activity patterns during encoding and recall  
434 (see Methods)<sup>50</sup>. We repeated this for Aversive encoding and correlated it with activity patterns during  
435 Aversive recall. Consistent with our hypothesis, Neutral encoding-to-recall correlations were lower in  
436 High Shock mice compared to Low Shock mice. In High Shock mice, the Neutral encoding-to-recall  
437 correlations were also lower than Aversive encoding-to-recall correlations, suggesting that the neutral  
438 memory representation was significantly altered from encoding to recall in High Shock mice (Figure  
439 4E). These results collectively suggest that a strong aversive experience drove the Neutral  $\cap$  Aversive  
440 and Neutral ensembles to co-fire during the offline period, altering the neutral memory representation.  
441 And during Neutral recall, these ensembles were again co-reactivated, leading to the enhanced  
442 freezing observed in the Neutral context.

443 **Figure 4**



444 **Figure 4. Strong aversive experience drives Neutral  $\cap$  Aversive ensemble reactivation during Neutral**  
445 **context recall.**

- 446  
447 A) Behavioral schematic of calcium imaging experiment, as in Figure 1D. Here, we focused on hippocampal  
448 activity during the Aversive, Neutral, and Novel recall sessions.  
449
- 450 B) Cells active only during the Neutral experience and not the Aversive experience were more likely to be  
451 reactivated when mice were placed back in the Neutral context, compared to when they were placed in a Novel  
452 context ( $F_{1,12} = 24.44$ ,  $p = 0.0003$ ). There was no effect of shock amplitude ( $F_{1,12} = 3.08$ ,  $p = 0.10$ ) (Low Shock,  $N$   
453  $= 6$  mice; High Shock,  $N = 8$  mice).  
454
- 455 C) Cells active during the Aversive experience and not the Neutral experience were no differently reactivated in  
456 Neutral vs Novel contexts. (Amplitude:  $F_{1,12} = 0.029$ ,  $p = 0.869$ ; Context:  $F_{1,12} = 1.39$ ,  $p = 0.261$ ; Amplitude x  
457 Context:  $F_{1,12} = 0.14$ ,  $p = 0.71$ ) (Low Shock,  $N = 6$  mice; High Shock,  $N = 8$  mice).  
458
- 459 D) Cells active during both the initial Neutral and Aversive experiences were subsequently more likely to be  
460 reactivated in the Neutral context compared to Novel context in High Shock mice ( $t_7 = 8.53$ ,  $p = 0.00012$ ), but not  
461 Low Shock mice ( $t_5 = 0.55$ ,  $p = 0.61$ ; Context x Amplitude:  $F_{1,12} = 10.33$ ,  $p = 0.007$ ) (Low Shock,  $N = 6$  mice; High  
462 Shock,  $N = 8$  mice).  
463
- 464 E) In High Shock mice, population activity patterns in the Neutral context changed significantly from Neutral  
465 encoding to Neutral recall (Amplitude:  $F_{1,12} = 5.65$ ; SessionPair:  $F_{1,12} = 10.42$ ; Amplitude x SessionPair:  $F_{1,12} =$   
466  $6.22$ ). During Neutral recall in High Shock mice, population activity vectors were less correlated with the average  
467 Neutral encoding population vector than Aversive recall activity was with the average Aversive encoding  
468 population vector ( $t_7 = 4.10$ ,  $p = 0.009$ ). Neutral encoding-to-recall correlations were also lower in High vs Low  
469 Shock mice ( $t_{6,92} = 2.98$ ,  $p = 0.042$ ). Aversive encoding-to-recall correlations were no different in High vs Low  
470 Shock mice ( $t_{6,11} = 1.13$ ,  $p = 0.30$ ). In Low Shock mice, Neutral and Aversive encoding-to-recall correlations were  
471 no different ( $t_5 = 0.23$ ,  $p = 0.83$ ) (Low Shock,  $N = 6$  mice; High Shock,  $N = 8$  mice).

## 472 Discussion

473 How animals actively update memories as they encounter new information remains a  
474 fundamental question in neuroscience<sup>21</sup>. Past work has shown that individual experiences are encoded  
475 by subpopulations of neurons across the brain that are highly active during learning<sup>51,52</sup>. These  
476 neuronal ensembles undergo synaptic modifications after learning to support memory storage<sup>53-56</sup>. After  
477 learning, activity of these ensembles is necessary<sup>38,57</sup> and sufficient<sup>2</sup> to drive memory recall, and their  
478 reactivation during memory recall is correlated with the strength of memory recall<sup>1</sup>. How memories  
479 encoded across time are integrated remains a critical and unanswered question in neuroscience. The  
480 memory allocation hypothesis suggests that neurons with high intrinsic excitability at the time of  
481 learning are likely to be allocated to a memory trace<sup>5,58</sup>. Prior studies suggest that two memories  
482 encoded within a day are likely to be linked because they share an overlapping population of highly  
483 excitable neurons during the initial learning. This shared neural ensemble links the two temporally  
484 related memories, such that the recall of one memory is more likely to trigger the recall of another  
485 memory that was encoded close in time<sup>4,27,28,59</sup>. Here we demonstrate that memories can be  
486 dynamically updated even days after they have been encoded and consolidated, and that this process  
487 is driven by ensemble co-reactivation during a post-learning period.

488 Whether linking memories across days is an adaptive or maladaptive process may depend on  
489 the environmental conditions. Under everyday circumstances, memories that are encoded far apart in  
490 time and which share no features in common may typically not need to be linked, and memories must  
491 also be segregated to allow for proper recall of distinct memories. Notably, the hippocampus has been  
492 shown to successfully discriminate between distinct memories<sup>60,61</sup>. However, after a potentially life-  
493 threatening experience, especially one where the source of the aversive outcome is ambiguous (as in  
494 the aversive experience employed here), it could benefit an animal to link fear from that aversive  
495 experience to prior events, particularly if the event is rare and novel as seen in conditioned taste  
496 aversion<sup>22</sup>. Our results suggest that a highly aversive experience is more likely to drive memory-linking  
497 than a mild aversive experience (Figure 1D-G), consistent with this intuition. Moreover, our results  
498 suggest that fear is more likely to be linked retrospectively to past events rather than prospectively to  
499 future events (Figure 1A-C). This is consistent with the notion that cues that occurred before an

500 outcome can predict that outcome. On a shorter timescale, it has been well established that when a  
501 neutral cue directly precedes a foot shock by seconds, this drives associative learning between the cue  
502 and the foot shock to drive cue-elicited freezing<sup>62,63</sup>. Interestingly, however, if the cue instead occurs  
503 directly *after* the foot shock, the animal no longer freezes in response to cue presentation thereafter,  
504 presumably because the cue predicts the ensuing absence of the aversive event<sup>64</sup>. Though the  
505 difference in timescale suggests that different mechanisms are likely at play in these two scenarios, our  
506 results are consistent with the idea that cues occurring prior to an outcome can be interpreted as  
507 predictive cues to the animal. A recent review has also suggested that animals use “retrospective  
508 cognitive maps” to infer the states that precede an outcome, to draw causal associations between  
509 those stimuli<sup>65</sup>. Our results suggest that offline periods are responsible for driving this retrospective  
510 inference (Figure 5).

511         Offline periods offer an opportunity for the brain to draw inferences about relationships that were  
512 not necessarily formed at the time of learning. In humans, it has been shown that an emotional  
513 experience can retrospectively increase memory for previously experienced neutral objects, only after a  
514 period of consolidation<sup>31</sup>. A separate study demonstrated that this retrospective memory enhancement  
515 coincided with increased functional hippocampal-cortical coupling and fMRI BOLD activity in the ventral  
516 tegmental area<sup>35</sup>. Moreover, a recent study in mice showed that two contexts with strongly shared  
517 geometrical features can be integrated immediately after learning (i.e., 15min after learning), whereas  
518 two contexts with subtly shared geometrical features require an offline period after learning (i.e., 1 day)  
519 to drive their integration. During this offline period, cortical ensemble co-reactivation drives this memory  
520 integration<sup>66</sup>. Our study demonstrates that a highly aversive experience can alter the likelihood of  
521 retrospective memory-linking, that this is dependent upon post-learning hippocampal activity, and is  
522 accompanied by co-reactivation of the ensembles for the two memories.

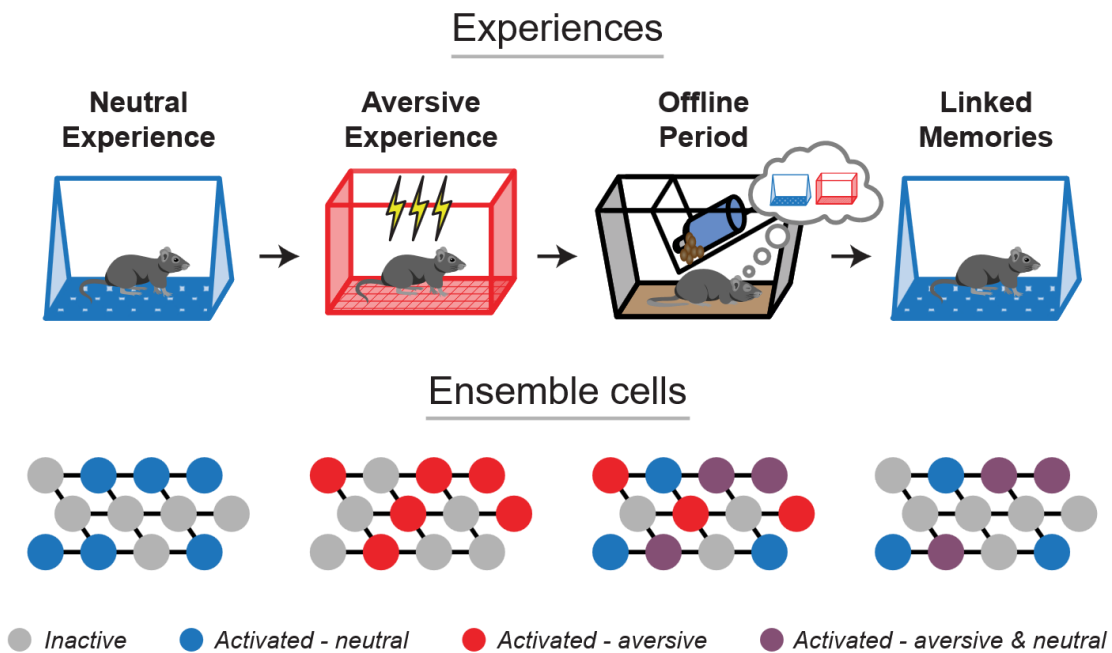
523         Past studies have shown that ensemble reactivation occurs during both sleep (NREM and REM  
524 sleep) and wake states. Reactivation during different states have been proposed to support different  
525 memory processes. For instance, classical studies demonstrated that following a salient experience,  
526 the patterns of neuronal activity that were present during learning are replayed in the same sequential  
527 order offline, and this replay has been observed during both NREM<sup>9</sup> and REM<sup>8</sup> sleep. The replay

528 observed during sleep was proposed to support memory consolidation, and indeed, disruption of sharp-  
529 wave ripples (during which most of these replay events occur) disrupts the storage of memories such  
530 that memory recall is disrupted thereafter<sup>16,19</sup>. Remarkably, one study found that prolonging sharp wave  
531 ripple durations benefited memory while cutting them short impaired memory<sup>67</sup>. In addition to sleep, it  
532 has also been observed that hippocampal replay occurs while animals are awake and engaged in an  
533 experimental task, and it can occur in a forward or reverse direction<sup>10,12,68,69</sup>. This has led to the idea  
534 that different forms of replay may serve different functions, from memory consolidation to planning and  
535 decision-making<sup>18,39</sup>, though this remains a debate<sup>70</sup>. More generally, sleep has been shown to strongly  
536 benefit learning in both rodents<sup>17,33,34,71</sup> and in humans<sup>32,72-74</sup>, and neurophysiological events during  
537 sleep, such as sharp wave ripples and sleep spindles, have been suggested to support memory  
538 consolidation<sup>16,19,71</sup>. Whether ensemble *co-reactivation* supporting memory integration is a sleep state  
539 specific phenomenon and whether distinct sleep/wake states differentially support memory  
540 consolidation versus integration has yet to be answered. Our results suggest that the transient  
541 population bursts during which we observed ensemble co-reactivation occurs during quiet wake, since  
542 locomotion decreased about one-second prior to each burst and resumed one-second following it  
543 (Extended Figure 5I,J). However, this study did not explicitly measure ensemble reactivation during  
544 distinct sleep states – thus, it remains unclear whether ensemble co-reactivation may occur in a sleep  
545 state specific manner to drive memory-linking. A recent study demonstrated that in a neural network  
546 model with autonomous offline reactivation, interleaved periods of NREM and REM sleep were critical  
547 for the integration of memories<sup>25</sup>. However, a previous study in rats suggested that offline reactivation  
548 and modification of a past neutral memory occurred during wake periods<sup>24</sup>. Thus, resolving whether  
549 and how different sleep states support memory integration processes will be an important future  
550 direction.

551 Finally, these results have implications for the interpretation of the clinical manifestation of  
552 memory-related conditions such as post-traumatic stress disorder (PTSD). PTSD transpires from one  
553 or multiple traumatic events and is hallmarked by uncontrollable fear in non-life-threatening contexts<sup>75</sup>.  
554 A common form of behavioral treatment for PTSD is exposure therapy, whereby the patient is carefully  
555 re-exposed to the trauma-associated conditioned stimuli, seeking to detach the association between

556 those stimuli and fear. In many cases, exposure therapy successfully decreases fear, but patients are  
557 often prone to relapse thereafter<sup>76</sup>. Our results suggest that highly salient aversive experiences can  
558 drive fear to be associated with seemingly unrelated stimuli that were not present at the time of the  
559 aversive experience, and that this scales with the perceived aversiveness of the experience (Figure  
560 1G). This predicts that while exposure therapy may successfully inhibit fear to the trauma stimuli, the  
561 fear from the trauma may have spread to other stimuli that were not directly targeted by the therapy.  
562 Thus, it may be useful to consider stimuli that were experienced across time that may have insidiously  
563 become linked with the trauma. Ultimately, our results point to the offline period after an aversive event  
564 as a potential intervention timepoint to unlink memories separated across days.

## 565 **Figure 5**



566 **Figure 5. Offline ensemble reactivation drives retrospective memory-linking across days.** After single  
567 experiences, the cells active during learning are reactivated to support their consolidation. After a strong aversive  
568 experience, memories are linked retrospectively across days by the co-reactivation of the ensembles representing  
569 both the recent and the past neutral memory ensembles. During recall of the neutral memory, many of the cells  
570 that were active during both the neutral and aversive experiences are reactivated to drive fear in the neutral  
571 context.



## 572 **References**

- 573
- 574 1 Reijmers, L. G., Perkins, B. L., Matsuo, N. & Mayford, M. Localization of a stable neural  
575 correlate of associative memory. *Science* **317**, 1230-1233 (2007).  
576 <https://doi.org/10.1126/science.1143839>
- 577 2 Liu, X. *et al.* Optogenetic stimulation of a hippocampal engram activates fear memory recall.  
578 *Nature* **484**, 381-385 (2012). <https://doi.org/10.1038/nature11028>
- 579 3 Han, J. H. *et al.* Neuronal competition and selection during memory formation. *Science* **316**,  
580 457-460 (2007). <https://doi.org/10.1126/science.1139438>
- 581 4 Rogerson, T. *et al.* Synaptic tagging during memory allocation. *Nat Rev Neurosci* **15**, 157-169  
582 (2014). <https://doi.org/10.1038/nrn3667>
- 583 5 Josselyn, S. A. & Frankland, P. W. Memory Allocation: Mechanisms and Function. *Annu Rev*  
584 *Neurosci* **41**, 389-413 (2018). <https://doi.org/10.1146/annurev-neuro-080317-061956>
- 585 6 Pavlides, C. & Winson, J. Influences of hippocampal place cell firing in the awake state on the  
586 activity of these cells during subsequent sleep episodes. *J Neurosci* **9**, 2907-2918 (1989).  
587 <https://doi.org/10.1523/JNEUROSCI.09-08-02907.1989>
- 588 7 Wilson, M. A. & McNaughton, B. L. Reactivation of hippocampal ensemble memories during  
589 sleep. *Science* **265**, 676-679 (1994). <https://doi.org/10.1126/science.8036517>
- 590 8 Louie, K. & Wilson, M. A. Temporally structured replay of awake hippocampal ensemble activity  
591 during rapid eye movement sleep. *Neuron* **29**, 145-156 (2001). [https://doi.org/10.1016/s0896-](https://doi.org/10.1016/s0896-6273(01)00186-6)  
592 [6273\(01\)00186-6](https://doi.org/10.1016/s0896-6273(01)00186-6)
- 593 9 Lee, A. K. & Wilson, M. A. Memory of sequential experience in the hippocampus during slow  
594 wave sleep. *Neuron* **36**, 1183-1194 (2002). [https://doi.org/10.1016/s0896-6273\(02\)01096-6](https://doi.org/10.1016/s0896-6273(02)01096-6)
- 595 10 Foster, D. J. & Wilson, M. A. Reverse replay of behavioural sequences in hippocampal place  
596 cells during the awake state. *Nature* **440**, 680-683 (2006). <https://doi.org/10.1038/nature04587>
- 597 11 Ji, D. & Wilson, M. A. Coordinated memory replay in the visual cortex and hippocampus during  
598 sleep. *Nat Neurosci* **10**, 100-107 (2007). <https://doi.org/10.1038/nn1825>
- 599 12 Diba, K. & Buzsaki, G. Forward and reverse hippocampal place-cell sequences during ripples.  
600 *Nat Neurosci* **10**, 1241-1242 (2007). <https://doi.org/10.1038/nn1961>

- 601 13 Carr, M. F., Jadhav, S. P. & Frank, L. M. Hippocampal replay in the awake state: a potential  
602 substrate for memory consolidation and retrieval. *Nat Neurosci* **14**, 147-153 (2011).  
603 <https://doi.org/10.1038/nn.2732>
- 604 14 Girardeau, G., Inema, I. & Buzsaki, G. Reactivations of emotional memory in the hippocampus-  
605 amygdala system during sleep. *Nat Neurosci* **20**, 1634-1642 (2017).  
606 <https://doi.org/10.1038/nn.4637>
- 607 15 Ghandour, K. *et al.* Orchestrated ensemble activities constitute a hippocampal memory engram.  
608 *Nat Commun* **10**, 2637 (2019). <https://doi.org/10.1038/s41467-019-10683-2>
- 609 16 Gridchyn, I., Schoenenberger, P., O'Neill, J. & Csicsvari, J. Assembly-Specific Disruption of  
610 Hippocampal Replay Leads to Selective Memory Deficit. *Neuron* **106**, 291-300 e296 (2020).  
611 <https://doi.org/10.1016/j.neuron.2020.01.021>
- 612 17 Clawson, B. C. *et al.* Causal role for sleep-dependent reactivation of learning-activated sensory  
613 ensembles for fear memory consolidation. *Nat Commun* **12**, 1200 (2021).  
614 <https://doi.org/10.1038/s41467-021-21471-2>
- 615 18 Buzsaki, G. Hippocampal sharp wave-ripple: A cognitive biomarker for episodic memory and  
616 planning. *Hippocampus* **25**, 1073-1188 (2015). <https://doi.org/10.1002/hipo.22488>
- 617 19 van de Ven, G. M., Trouche, S., McNamara, C. G., Allen, K. & Dupret, D. Hippocampal Offline  
618 Reactivation Consolidates Recently Formed Cell Assembly Patterns during Sharp Wave-  
619 Ripples. *Neuron* **92**, 968-974 (2016). <https://doi.org/10.1016/j.neuron.2016.10.020>
- 620 20 Colgin, L. L. Rhythms of the hippocampal network. *Nat Rev Neurosci* **17**, 239-249 (2016).  
621 <https://doi.org/10.1038/nrn.2016.21>
- 622 21 Mau, W., Hasselmo, M. E. & Cai, D. J. The brain in motion: How ensemble fluidity drives  
623 memory-updating and flexibility. *Elife* **9** (2020). <https://doi.org/10.7554/eLife.63550>
- 624 22 Chambers, K. C. Conditioned taste aversions. *World J Otorhinolaryngol Head Neck Surg* **4**, 92-  
625 100 (2018). <https://doi.org/10.1016/j.wjorl.2018.02.003>
- 626 23 Cai, D. J., Mednick, S. A., Harrison, E. M., Kanady, J. C. & Mednick, S. C. REM, not incubation,  
627 improves creativity by priming associative networks. *Proc Natl Acad Sci U S A* **106**, 10130-  
628 10134 (2009). <https://doi.org/10.1073/pnas.0900271106>

- 629 24 Jezek, K. *et al.* Stress-induced out-of-context activation of memory. *PLoS Biol* **8**, e1000570  
630 (2010). <https://doi.org/10.1371/journal.pbio.1000570>
- 631 25 Singh, D., Norman, K. A. & Schapiro, A. C. A model of autonomous interactions between  
632 hippocampus and neocortex driving sleep-dependent memory consolidation. *Proc Natl Acad Sci*  
633 *U S A* **119**, e2123432119 (2022). <https://doi.org/10.1073/pnas.2123432119>
- 634 26 Kurth-Nelson, Z. *et al.* Replay and compositional computation. *Neuron* (2023).  
635 <https://doi.org/10.1016/j.neuron.2022.12.028>
- 636 27 Cai, D. J. *et al.* A shared neural ensemble links distinct contextual memories encoded close in  
637 time. *Nature* **534**, 115-118 (2016). <https://doi.org/10.1038/nature17955>
- 638 28 Rashid, A. J. *et al.* Competition between engrams influences fear memory formation and recall.  
639 *Science* **353**, 383-387 (2016). <https://doi.org/10.1126/science.aaf0594>
- 640 29 Phelps, E. A. & Sharot, T. How (and Why) Emotion Enhances the Subjective Sense of  
641 Recollection. *Curr Dir Psychol Sci* **17**, 147-152 (2008). [https://doi.org/10.1111/j.1467-](https://doi.org/10.1111/j.1467-8721.2008.00565.x)  
642 [8721.2008.00565.x](https://doi.org/10.1111/j.1467-8721.2008.00565.x)
- 643 30 LaBar, K. S. & Cabeza, R. Cognitive neuroscience of emotional memory. *Nat Rev Neurosci* **7**,  
644 54-64 (2006). <https://doi.org/10.1038/nrn1825>
- 645 31 Dunsmoor, J. E., Murty, V. P., Davachi, L. & Phelps, E. A. Emotional learning selectively and  
646 retroactively strengthens memories for related events. *Nature* **520**, 345-348 (2015).  
647 <https://doi.org/10.1038/nature14106>
- 648 32 Diekelmann, S. & Born, J. The memory function of sleep. *Nat Rev Neurosci* **11**, 114-126 (2010).  
649 <https://doi.org/10.1038/nrn2762>
- 650 33 Havekes, R. *et al.* Sleep deprivation causes memory deficits by negatively impacting neuronal  
651 connectivity in hippocampal area CA1. *Elife* **5** (2016). <https://doi.org/10.7554/eLife.13424>
- 652 34 Cai, D. J., Shuman, T., Gorman, M. R., Sage, J. R. & Anagnostaras, S. G. Sleep selectively  
653 enhances hippocampus-dependent memory in mice. *Behav Neurosci* **123**, 713-719 (2009).  
654 <https://doi.org/10.1037/a0016415>
- 655 35 Clewett, D., Dunsmoor, J., Bachman, S. L., Phelps, E. A. & Davachi, L. Survival of the salient:  
656 Aversive learning rescues otherwise forgettable memories via neural reactivation and post-

- 657 encoding hippocampal connectivity. *Neurobiol Learn Mem* **187**, 107572 (2022).  
658 <https://doi.org/10.1016/j.nlm.2021.107572>
- 659 36 Lewis, P. A., Knoblich, G. & Poe, G. How Memory Replay in Sleep Boosts Creative Problem-  
660 Solving. *Trends Cogn Sci* **22**, 491-503 (2018). <https://doi.org/10.1016/j.tics.2018.03.009>
- 661 37 Bittner, K. C., Milstein, A. D., Grienberger, C., Romani, S. & Magee, J. C. Behavioral time scale  
662 synaptic plasticity underlies CA1 place fields. *Science* **357**, 1033-1036 (2017).  
663 <https://doi.org/10.1126/science.aan3846>
- 664 38 Denny, C. A. *et al.* Hippocampal memory traces are differentially modulated by experience,  
665 time, and adult neurogenesis. *Neuron* **83**, 189-201 (2014).  
666 <https://doi.org/10.1016/j.neuron.2014.05.018>
- 667 39 Joo, H. R. & Frank, L. M. The hippocampal sharp wave-ripple in memory retrieval for immediate  
668 use and consolidation. *Nat Rev Neurosci* **19**, 744-757 (2018). [https://doi.org/10.1038/s41583-](https://doi.org/10.1038/s41583-018-0077-1)  
669 [018-0077-1](https://doi.org/10.1038/s41583-018-0077-1)
- 670 40 Magnus, C. J. *et al.* Chemical and genetic engineering of selective ion channel-ligand  
671 interactions. *Science* **333**, 1292-1296 (2011). <https://doi.org/10.1126/science.1206606>
- 672 41 Ghandour, K. & Inokuchi, K. Memory reactivations during sleep. *Neurosci Res* (2022).  
673 <https://doi.org/10.1016/j.neures.2022.12.018>
- 674 42 Malvache, A., Reichinnek, S., Villette, V., Haimerl, C. & Cossart, R. Awake hippocampal  
675 reactivations project onto orthogonal neuronal assemblies. *Science* **353**, 1280-1283 (2016).  
676 <https://doi.org/10.1126/science.aaf3319>
- 677 43 Villette, V., Malvache, A., Tressard, T., Dupuy, N. & Cossart, R. Internally Recurring  
678 Hippocampal Sequences as a Population Template of Spatiotemporal Information. *Neuron* **88**,  
679 357-366 (2015). <https://doi.org/10.1016/j.neuron.2015.09.052>
- 680 44 Buzsaki, G. Neural syntax: cell assemblies, synapsesembles, and readers. *Neuron* **68**, 362-385  
681 (2010). <https://doi.org/10.1016/j.neuron.2010.09.023>
- 682 45 Rajasethupathy, P. *et al.* Projections from neocortex mediate top-down control of memory  
683 retrieval. *Nature* **526**, 653-659 (2015). <https://doi.org/10.1038/nature15389>

- 684 46 Gava, G. P. *et al.* Integrating new memories into the hippocampal network activity space. *Nat*  
685 *Neurosci* **24**, 326-330 (2021). [https://doi.org:10.1038/s41593-021-00804-w](https://doi.org/10.1038/s41593-021-00804-w)
- 686 47 Buzsaki, G. & Mizuseki, K. The log-dynamic brain: how skewed distributions affect network  
687 operations. *Nat Rev Neurosci* **15**, 264-278 (2014). [https://doi.org:10.1038/nrn3687](https://doi.org/10.1038/nrn3687)
- 688 48 Luccioli, S., Ben-Jacob, E., Barzilai, A., Bonifazi, P. & Torcini, A. Clique of functional hubs  
689 orchestrates population bursts in developmentally regulated neural networks. *PLoS Comput Biol*  
690 **10**, e1003823 (2014). [https://doi.org:10.1371/journal.pcbi.1003823](https://doi.org/10.1371/journal.pcbi.1003823)
- 691 49 Rolls, E. T. The mechanisms for pattern completion and pattern separation in the hippocampus.  
692 *Front Syst Neurosci* **7**, 74 (2013). [https://doi.org:10.3389/fnsys.2013.00074](https://doi.org/10.3389/fnsys.2013.00074)
- 693 50 Zaki, Y. *et al.* Hippocampus and amygdala fear memory engrams re-emerge after contextual  
694 fear relapse. *Neuropsychopharmacology* **47**, 1992-2001 (2022). [https://doi.org:10.1038/s41386-](https://doi.org/10.1038/s41386-022-01407-0)  
695 [022-01407-0](https://doi.org/10.1038/s41386-022-01407-0)
- 696 51 Josselyn, S. A. & Tonegawa, S. Memory engrams: Recalling the past and imagining the future.  
697 *Science* **367** (2020). [https://doi.org:10.1126/science.aaw4325](https://doi.org/10.1126/science.aaw4325)
- 698 52 Zhou, Y. *et al.* CREB regulates excitability and the allocation of memory to subsets of neurons  
699 in the amygdala. *Nat Neurosci* **12**, 1438-1443 (2009). [https://doi.org:10.1038/nn.2405](https://doi.org/10.1038/nn.2405)
- 700 53 Bocchio, M., Nabavi, S. & Capogna, M. Synaptic Plasticity, Engrams, and Network Oscillations  
701 in Amygdala Circuits for Storage and Retrieval of Emotional Memories. *Neuron* **94**, 731-743  
702 (2017). [https://doi.org:10.1016/j.neuron.2017.03.022](https://doi.org/10.1016/j.neuron.2017.03.022)
- 703 54 Ryan, T. J., Roy, D. S., Pignatelli, M., Arons, A. & Tonegawa, S. Memory. Engram cells retain  
704 memory under retrograde amnesia. *Science* **348**, 1007-1013 (2015).  
705 [https://doi.org:10.1126/science.aaa5542](https://doi.org/10.1126/science.aaa5542)
- 706 55 Choi, J. H. *et al.* Interregional synaptic maps among engram cells underlie memory formation.  
707 *Science* **360**, 430-435 (2018). [https://doi.org:10.1126/science.aas9204](https://doi.org/10.1126/science.aas9204)
- 708 56 Abdou, K. *et al.* Synapse-specific representation of the identity of overlapping memory engrams.  
709 *Science* **360**, 1227-1231 (2018). [https://doi.org:10.1126/science.aat3810](https://doi.org/10.1126/science.aat3810)
- 710 57 Han, J. H. *et al.* Selective erasure of a fear memory. *Science* **323**, 1492-1496 (2009).  
711 [https://doi.org:10.1126/science.1164139](https://doi.org/10.1126/science.1164139)

- 712 58 Silva, A. J., Zhou, Y., Rogerson, T., Shobe, J. & Balaji, J. Molecular and cellular approaches to  
713 memory allocation in neural circuits. *Science* **326**, 391-395 (2009).  
714 <https://doi.org/10.1126/science.1174519>
- 715 59 Yokose, J. *et al.* Overlapping memory trace indispensable for linking, but not recalling, individual  
716 memories. *Science* **355**, 398-403 (2017). <https://doi.org/10.1126/science.aal2690>
- 717 60 van Dijk, M. T. & Fenton, A. A. On How the Dentate Gyrus Contributes to Memory  
718 Discrimination. *Neuron* **98**, 832-845 e835 (2018). <https://doi.org/10.1016/j.neuron.2018.04.018>
- 719 61 Lohnas, L. J. *et al.* Time-resolved neural reinstatement and pattern separation during memory  
720 decisions in human hippocampus. *Proc Natl Acad Sci U S A* **115**, E7418-E7427 (2018).  
721 <https://doi.org/10.1073/pnas.1717088115>
- 722 62 LeDoux, J. E. Emotion circuits in the brain. *Annu Rev Neurosci* **23**, 155-184 (2000).  
723 <https://doi.org/10.1146/annurev.neuro.23.1.155>
- 724 63 Maren, S. Neurobiology of Pavlovian fear conditioning. *Annu Rev Neurosci* **24**, 897-931 (2001).  
725 <https://doi.org/10.1146/annurev.neuro.24.1.897>
- 726 64 Moscovitch, A. & LoLordo, V. M. Role of safety in the Pavlovian backward fear conditioning  
727 procedure. *J Comp Physiol Psychol* **66**, 673-678 (1968). <https://doi.org/10.1037/h0026548>
- 728 65 VM, K. N. & Stuber, G. D. The learning of prospective and retrospective cognitive maps within  
729 neural circuits. *Neuron* **109**, 3552-3575 (2021). <https://doi.org/10.1016/j.neuron.2021.09.034>
- 730 66 Aly, M. H., Abdou, K., Okubo-Suzuki, R., Nomoto, M. & Inokuchi, K. Selective engram  
731 coreactivation in idling brain inspires implicit learning. *Proc Natl Acad Sci U S A* **119**,  
732 e2201578119 (2022). <https://doi.org/10.1073/pnas.2201578119>
- 733 67 Fernandez-Ruiz, A. *et al.* Long-duration hippocampal sharp wave ripples improve memory.  
734 *Science* **364**, 1082-1086 (2019). <https://doi.org/10.1126/science.aax0758>
- 735 68 Karlsson, M. P. & Frank, L. M. Awake replay of remote experiences in the hippocampus. *Nat*  
736 *Neurosci* **12**, 913-918 (2009). <https://doi.org/10.1038/nn.2344>
- 737 69 Jackson, J. C., Johnson, A. & Redish, A. D. Hippocampal sharp waves and reactivation during  
738 awake states depend on repeated sequential experience. *J Neurosci* **26**, 12415-12426 (2006).  
739 <https://doi.org/10.1523/JNEUROSCI.4118-06.2006>

- 740 70 Gillespie, A. K. *et al.* Hippocampal replay reflects specific past experiences rather than a plan  
741 for subsequent choice. *Neuron* **109**, 3149-3163 e3146 (2021).  
742 <https://doi.org/10.1016/j.neuron.2021.07.029>
- 743 71 Varga, A. W., Kang, M., Ramesh, P. V. & Klann, E. Effects of acute sleep deprivation on motor  
744 and reversal learning in mice. *Neurobiol Learn Mem* **114**, 217-222 (2014).  
745 <https://doi.org/10.1016/j.nlm.2014.07.001>
- 746 72 Denis, D. *et al.* The roles of item exposure and visualization success in the consolidation of  
747 memories across wake and sleep. *Learn Mem* **27**, 451-456 (2020).  
748 <https://doi.org/10.1101/lm.051383.120>
- 749 73 Wagner, U., Gais, S., Haider, H., Verleger, R. & Born, J. Sleep inspires insight. *Nature* **427**,  
750 352-355 (2004). <https://doi.org/10.1038/nature02223>
- 751 74 Klinzing, J. G., Niethard, N. & Born, J. Mechanisms of systems memory consolidation during  
752 sleep. *Nat Neurosci* **22**, 1598-1610 (2019). <https://doi.org/10.1038/s41593-019-0467-3>
- 753 75 Ressler, K. J. *et al.* Post-traumatic stress disorder: clinical and translational neuroscience from  
754 cells to circuits. *Nat Rev Neurol* **18**, 273-288 (2022). [https://doi.org/10.1038/s41582-022-00635-](https://doi.org/10.1038/s41582-022-00635-8)  
755 [8](https://doi.org/10.1038/s41582-022-00635-8)
- 756 76 Boschen, M. J., Neumann, D. L. & Waters, A. M. Relapse of successfully treated anxiety and  
757 fear: theoretical issues and recommendations for clinical practice. *Aust N Z J Psychiatry* **43**, 89-  
758 100 (2009). <https://doi.org/10.1080/00048670802607154>
- 759

## 762 **Methods**

### 763 Subjects

764 Adult C57BL/6J mice from Jackson Laboratories were used in all experiments. Mice arrived group-  
765 housed in cages of 4 mice/cage and were singly housed for the experiment. For behavioral  
766 experiments where mice did not undergo surgery, mice were ordered to arrive at 12 weeks of age and  
767 underwent behavioral testing 1-2 weeks from then. For experiments where mice underwent surgery,  
768 mice were ordered to arrive at 8-9 weeks of age and underwent behavioral testing about 4-6 weeks  
769 after the arrival date.

770

### 771 Viral constructs

772 For calcium imaging experiments, AAV1-Syn-GCaMP6f-WPRE-SV40 (titer:  $2.8 \times 10^{13}$  GC/mL) was  
773 purchased from AddGene and was diluted 1:4 in sterile 1x PBS. Mice had 300nL of the diluted virus  
774 injected into the right hemisphere of dorsal CA1. For PSAM experiments, AAV5-Syn-PSAM4-GlyR-  
775 IRES-eGFP ( $2.4 \times 10^{13}$  GC/mL) was purchased from AddGene. Mice had the virus injected at stock  
776 titer bilaterally into dorsal and ventral hippocampus, 300nL per injection site.

777

### 778 Surgery

779 Mice were anesthetized with 1 to 2% isoflurane for surgical procedures and placed into a stereotaxic  
780 frame (David Kopf Instruments, Tujunga, CA). Eye ointment was applied to prevent desiccation, and  
781 mice were kept on a heated pad to prevent hypothermia. Surgery was performed with aseptic  
782 technique. After surgery, carprofen (5 mg/kg) was administered every day for the following three days,  
783 and ampicillin (20 mg/kg) was administered every day for the following 7 days. For calcium imaging  
784 experiments, dexamethasone (0.2 mg/kg) was also administered for the following 7 days.

785

786 For PSAM experiments, AAV5-Syn-PSAM4-GlyR-IRES-eGFP was injected at stock concentration.  
787 Mice had 300nL of the virus injected bilaterally into dorsal hippocampus (AP: -2mm, ML: +/-1.5mm, DV:  
788 -1.5mm) and 300nL injected bilaterally into ventral hippocampus (AP: -3mm, ML: +/-3.2mm, DV: -  
789 4mm), for a total of 4 injections and 1.2uL injected per mouse, using a glass pipette and Nanoject



790 injector. The pipette was slowly lowered to the injection site, the virus was injected at 2nL/sec, and then  
791 the pipette remained for 5min before being removed to allow for virus diffusion. Mice had their incision  
792 sutured following surgery and had betadine applied to the site to prevent infection.

793  
794 For calcium imaging experiments, mice underwent two serial surgeries spaced one month apart, as  
795 described before<sup>1</sup>. During the first surgery, a 1mm diameter craniotomy was made above the dorsal  
796 hippocampus on the right hemisphere (centered at AP -2mm, ML +1.5mm from bregma). An anchor  
797 screw was screwed into the skull on the contralateral hemisphere at approximately AP -1mm and ML -  
798 2.5mm from bregma. 300nL of AAV1-Syn-GCaMP6f was injected into dorsal CA1 of the hippocampus  
799 on the right hemisphere (AP -2mm, ML +1.5mm, DV -1.2mm). Virus was injected as described in  
800 PSAM experiments above. After the pipette was removed, the mouse remained on the stereotaxic  
801 frame for 20min to allow for complete diffusion of the virus. After the 20min of diffusion, the cortex  
802 below the craniotomy was aspirated with a 25-gauge blunt syringe needle attached to a vacuum pump,  
803 while constantly being irrigated with cortex buffer. When the striations of the corpus callosum were  
804 visible, the 25-gauge needle was replaced with a 27-gauge needle for finer tuned aspiration. Once most  
805 of corpus callosum was removed, bleeding was controlled using surgical foam (Surgifoam), and then a  
806 1mm diameter x 4mm length GRIN lens (GRINTECH) was slowly lowered into the craniotomy. The lens  
807 was fixed with cyanoacrylate, and then dental acrylic was applied to cement the implant in place and  
808 cover the rest of the exposed skull. The top of the exposed lens was covered with Kwik-Sil (World  
809 Precision Instruments) to protect it and the Kwik-Sil was covered with dental cement. Four weeks later,  
810 mice were returned to attach the baseplate, visually guided by a Miniscope. The overlying dental  
811 cement was drilled off and the Kwik-Sil was removed to reveal the top of the lens. The Miniscope with  
812 an attached baseplate was lowered near the implanted lens and the field of view was monitored in real-  
813 time on a computer. The Miniscope was rotated until a well-exposed field of view was observed, at  
814 which point the baseplate was fixed to the implant with cyanoacrylate and dental cement. The mouse  
815 did not receive post-operative drugs after this surgery since it was not invasive.

816

817 Behavioral procedures

818 Prior to all experiments, mice were handled for one minute each day for at least one week. On at least  
819 four of those days, mice were transported to the testing room and handled there. On the rest of the  
820 days, the mice were handled in the vivarium. In calcium imaging experiments, mice were handled and  
821 habituated for 2 weeks instead of 1, during which they were habituated to having the Miniscope  
822 attached and detached from its head. To become accustomed to the weight of the Miniscope, they  
823 were placed in their homecage with the Miniscope attached for 5min per day for at least 5 days.  
824  
825 In Retrospective and Prospective memory-linking behavioral experiments, mice were exposed to the  
826 Neutral context for 10 minutes to explore. During Aversive encoding, mice were placed in a novel  
827 context and allowed to explore for 2 minutes. Then, mice received a 2-second foot shock of either  
828 0.25mA (low shock) or 1.5mA (high shock). One minute after the first shock, they received a second  
829 shock of the same duration and amplitude, with a third shock following 1 minute after the second. 30  
830 seconds after the third shock, the mice were removed and placed back in their homecage. On the  
831 following three days, mice were tested in the previously experienced Aversive and Neutral contexts, as  
832 well as a completely Novel context that they had not been exposed to prior. The features of the Neutral  
833 and Novel contexts were counter-balanced and were made up of different olfactory, auditory, lighting,  
834 and tactile cues. The Aversive context was always the same with distinct cues from the Neutral and  
835 Novel contexts. In the PSAM experiment, mice were tested in either the Aversive, Neutral, or Novel  
836 context. In the Prospective versus Retrospective memory-linking experiment, mice were tested in the  
837 Aversive context first, and then half the mice were tested in the Neutral context and the other half in the  
838 Novel context. In the Low vs High Shock experiments, mice were tested in the Aversive context first,  
839 followed by testing in the Neutral and Novel context counter-balanced; half the mice received Neutral  
840 recall and then Novel context exposure the next day, and the other half Novel context exposure and  
841 then Neutral recall. All testing was done in Med Associates chambers. Behavioral data were analyzed  
842 using the Med Associates software for measuring freezing. In experiments where mice were tethered  
843 with a Miniscope, behavioral data were analyzed using our previously published open-source  
844 behavioral tracking pipeline, ezTrack<sup>2</sup>. In the Prospective versus Retrospective memory-linking  
845 timecourse experiments, the Aversive learning experience was distinct: mice explored for 2min, then

846 administered one 0.75mA, 2-second long foot shock and removed from the context 30sec following this  
847 shock.

848

#### 849 Drug injections

850 uPSEM-817 tartrate was made in a solution of 0.1mg/mL in saline and injected intraperitoneally at a  
851 dose of 1mg/kg (10mL/kg injection volume). Saline was used as a vehicle. The first injection was done  
852 as soon as the mice were brought back to the vivarium after Aversive encoding (~3min after the end of  
853 Aversive encoding). The next 3 injections were done every 3 hours to cover a 12-hour timespan of  
854 inhibition.

855

#### 856 Calcium imaging Miniscope recordings

857 Open-source V4 Miniscopes (<https://github.com/Aharoni-Lab/Miniscope-v4>) were connected to a  
858 coaxial cable which connected to a Miniscope data acquisition board (DAQ) 3.3. The DAQ connected to  
859 a computer via a USB3.0. Data was collected via the Miniscope QT Software  
860 (<https://github.com/Aharoni-Lab/Miniscope-DAQ-QT-Software>) at 30 frames per second. Miniscopes  
861 and DAQ boards were all purchased from Open Ephys.

862

863 When performing calcium imaging with concurrent behavior in the Med Associates boxes, mice were  
864 brought into the testing room from the vivarium, taken out of their homecage, and had the Miniscope  
865 attached. They were placed back into their homecage for 1min. Then, they were removed from their  
866 homecage and placed in the testing chamber. To record calcium and behavior, the Med Associates  
867 software sent a continuous TTL pulse to record from the Miniscope while the behavior was concurrently  
868 tracked via Med Associates cameras. After the session was complete, the mice were immediately  
869 returned to their homecage, then the Miniscope was removed, and the mouse was returned to the  
870 vivarium. One mouse was brought to the testing room at a time so that mice did not idly wait in the  
871 testing room with partial recall cues from the room present.

872

873 Offline calcium imaging recordings were done in the mouse's homecage for the 1 hour following Neutral  
874 encoding and following Aversive encoding. During these recordings, mice were placed back in their  
875 homecage and the homecage was placed in a large rectangular and opaque storage bin to occlude  
876 distal cues, with a webcam (Logitech C920e) overlying the homecage to track behavior during the  
877 recording. Using the Miniscope QT Software with two devices connected (Miniscope and webcam),  
878 calcium imaging and behavior were concurrently tracked. After the offline recording was complete, mice  
879 were removed from their homecage, the Miniscope was removed, they were returned to their  
880 homecage and returned to the vivarium immediately thereafter. The same procedure was undergone  
881 for the experiment in Extended Figure 3.

882

### 883 Miniscope data processing and data alignment

884 To extract calcium transients from the calcium imaging data, we employed our previously published  
885 open-source calcium imaging data processing pipeline, Minian<sup>3</sup>. Briefly, videos were pre-processed for  
886 background fluorescence and sensor noise, and motion corrected. Then, putative cell bodies were  
887 detected to feed into a constrained non-negative matrix factorization algorithm to decompose the 3-  
888 dimensional video array into a 3-dimensional array representing the spatial footprint of each cell, as  
889 well as a 2-dimensional matrix representing the calcium transients of each cell. The calcium transients  
890 were then deconvolved to extract the estimated time of each calcium transient. These deconvolved  
891 calcium activities were analyzed in these studies, after undergoing various transformations depending  
892 on the specific analysis (see below). Cells recorded across sessions within a mouse were cross-  
893 registered using a previously published open-source cross-registration algorithm, CellReg, using the  
894 spatial correlations of nearby cells to determine whether highly correlated footprints close in space are  
895 likely to be the same cell across sessions<sup>4</sup>.

896

897 To align calcium imaging data with behavior, behavior recordings were first aligned to an idealized  
898 template assuming a perfect sampling rate. This meant that if a recording session was 5min long, this  
899 meant that there should be  $300\text{sec} * 30\text{frames/sec} = 9000\text{frames}$ . All behavior recordings were within 4  
900 frames of this perfect template. Calcium recordings recorded with a much more variable and dynamic

901 sampling rate. Then, for each behavior frame, the closest calcium imaging frame was aligned to that  
902 frame, using the computer timestamp of that frame in milliseconds. No calcium imaging frame was re-  
903 used more than twice.

904

#### 905 General statistics and code/data availability

906 All analyses and statistics were done using custom-written Python and R scripts. Code detailing all the  
907 analysis in this manuscript will be made available upon publication (<https://github.com/denisecailab>).  
908 Calcium imaging data used in this manuscript will be made available using the Neurodata Without  
909 Borders framework to seamlessly share data across institutions<sup>5</sup>. Statistical significance was assessed  
910 with two-tailed paired and unpaired t-tests, as well as one-way, two-way, or three-way ANOVAs, linear  
911 mixed effects models, or Chi-square test where appropriate. Significant effects or interaction were  
912 followed with post-hoc testing with the use of orthogonal contrasts or with Benjamini-Hochberg  
913 corrections for multiple comparisons. Significance levels were set to  $\alpha=0.05$ . Significance for  
914 comparisons: \* $p<0.05$ ; \*\* $p<0.01$ ; \*\*\* $p<0.001$ ; \*\*\*\* $p<0.0001$ . Sample sizes were chosen based on  
915 previous similar studies. The investigators were not blinded to behavioral testing in calcium imaging  
916 studies but were blinded to behavioral testing in all other experiments.

917

#### 918 Ensemble reactivation analysis

919 To measure ensemble reactivation across the offline period, for each mouse, the matrix of neural  
920 activity that was recorded during the offline session was z-scored along both axes (cells and time).  
921 Cells were then broken up into ensembles based on whether they were previously observed to be  
922 active. Previously active cells were defined based on whether they had a corresponding matched cell  
923 via CellReg. On Offline1 after Neutral encoding, cells were either previously matched to an active cell  
924 during Neutral encoding (Neutral ensemble) or had no previously matched cell (Remaining ensemble).  
925 On Offline2, cells had a matched cell only with Neutral encoding and not Aversive encoding (Neutral  
926 ensemble), a matched cell with Aversive encoding and not Neutral encoding (Aversive ensemble), a  
927 matched cell on both Neutral encoding and Aversive encoding (Neutral  $\cap$  Aversive ensemble), or no

928 matched cell (Remaining ensemble). For each ensemble, the activity of cells was averaged across  
929 cells, and then averaged across time for each timebin.

930

### 931 Burst participation analysis

932 To measure population bursts, for each mouse, all cells that were recorded during that session were z-  
933 scored along the time dimension, such that each cell was normalized to its own activity. By doing this,  
934 no cell overly contributed to population bursts by having a very high amplitude event. Then, the mean  
935 population activity across the whole population was computed across the session and that 1-  
936 dimensional trace was z-scored. Time periods when the mean population activity reached above a  
937 threshold of  $z=2$  were considered burst events. During each of these burst events, each cell was  
938 considered to have “participated” if its activity was above  $z=2$  during the event. For each ensemble (as  
939 defined in the previous section), the fraction of the ensemble that participated in each event was  
940 computed, and then this was averaged across all events. The average participation of each ensemble  
941 was compared across ensembles and across Low vs High Shock groups.

942

### 943 Ensemble co-participation analysis

944 To measure ensemble co-participation during bursts, first bursts were defined based on the z-scored  
945 mean population activity of the whole population. Then, for each burst event, the z-scored mean  
946 population activity was computed for the Neutral ensemble and for the Aversive ensemble (see  
947 *Ensemble reactivation analysis* for ensemble definitions). For each population-level burst event, the  
948 “participation” of the Neutral ensemble or Aversive ensemble was measured based on whether the  
949 ensemble’s mean population activity was above the  $z=2$  threshold during the population level event.  
950 The burst events where one ensemble participated without the other ensembles were considered  
951 independent participations. The burst events where multiple ensembles simultaneously participated in  
952 were considered co-participations. The fraction of burst events where each ensemble independently  
953 and co- participated in were computed. Then, the same computation was made for all non-burst periods  
954 to ask how frequently the ensembles burst independently and coincidentally outside of burst events.

955

956 Time-lagged cross-correlation analysis

957 To measure cross-correlations, first mean ensemble activities were computed for the Neutral  $\cap$   
958 Aversive, Neutral, and Aversive ensembles (see previous two sections). Then, each time series was  
959 broken up into 120 sec bins. The Neutral  $\cap$  Aversive ensemble was separately correlated with the  
960 Neutral ensemble and the Aversive ensemble bin by bin. For each time bin, cross-correlations were  
961 computed for lags up to a maximum of 5 frames (or ~160ms). The maximum correlation was taken for  
962 each time bin, and the average correlation across time bins was computed. This led to, for each mouse,  
963 an average correlation between the Neutral  $\cap$  Aversive ensemble and the Neutral ensemble, and an  
964 average correlation between the Neutral  $\cap$  Aversive ensemble and the Aversive ensemble, across the  
965 offline period.

966

967 Encoding-to-Recall population vector correlation analysis

968 To measure correlations between encoding and recall activity patterns, first for each mouse, only cells  
969 that were active during both the encoding and recall session were included in the analysis and were  
970 aligned across the two sessions. For the encoding session, the mean population activity across the  
971 entire session was computed to produce one vector. Then, the recall session was broken up into 30-  
972 second bins and the mean population activity vector was computed for each bin. The encoding vector  
973 was correlated with each recall vector, as described before<sup>6</sup>. Finally, the correlations across all the  
974 recall bins were averaged to produce one average correlation between encoding and recall, for each  
975 mouse.

976 **Methods References**

- 977 1 Cai, D. J. *et al.* A shared neural ensemble links distinct contextual memories encoded close in  
978 time. *Nature* **534**, 115-118 (2016). [https://doi.org:10.1038/nature17955](https://doi.org/10.1038/nature17955)
- 979 2 Pennington, Z. T. *et al.* ezTrack: An open-source video analysis pipeline for the investigation of  
980 animal behavior. *Sci Rep* **9**, 19979 (2019). [https://doi.org:10.1038/s41598-019-56408-9](https://doi.org/10.1038/s41598-019-56408-9)
- 981 3 Dong, Z. *et al.* Minian, an open-source miniscope analysis pipeline. *Elife* **11** (2022).  
982 [https://doi.org:10.7554/eLife.70661](https://doi.org/10.7554/eLife.70661)
- 983 4 Sheintuch, L. *et al.* Tracking the Same Neurons across Multiple Days in Ca(2+) Imaging Data.  
984 *Cell Rep* **21**, 1102-1115 (2017). [https://doi.org:10.1016/j.celrep.2017.10.013](https://doi.org/10.1016/j.celrep.2017.10.013)
- 985 5 Rubel, O. *et al.* The Neurodata Without Borders ecosystem for neurophysiological data science.  
986 *Elife* **11** (2022). [https://doi.org:10.7554/eLife.78362](https://doi.org/10.7554/eLife.78362)
- 987 6 Zaki, Y. *et al.* Hippocampus and amygdala fear memory engrams re-emerge after contextual  
988 fear relapse. *Neuropsychopharmacology* **47**, 1992-2001 (2022). [https://doi.org:10.1038/s41386-](https://doi.org/10.1038/s41386-022-01407-0)  
989 [022-01407-0](https://doi.org/10.1038/s41386-022-01407-0)
- 990



991 **Acknowledgments**

992 This work was supported by the DP2 MH122399, R01 MH120162, Brain Research Foundation Award,  
993 Klingenstein-Simons Fellowship, NARSAD Young Investigator Award, McKnight Memory and Cognitive  
994 Disorder Award, One Mind-Otsuka Rising Star Research Award, Hirschl/Weill-Caulier Award, Mount  
995 Sinai Distinguished Scholar Award, and Friedman Brain Institute Award, to DJC; the CURE Taking  
996 Flight Award, American Epilepsy Society Junior Investigator Award, R03 NS111493, R21 DA049568,  
997 R01NS116357, RF1AG072497 to TS; NIMH F31MH126543 to YZ; NIMH K99 MH131792 and BBRF  
998 Young Investigator Award to ZTP; NIMH R01 MH113071, NIA R01 AG013622, and Dr. Miriam and  
999 Sheldon G. Adelson Medical Research Foundation to AJS; F32NS116416 to ZCW. We would like to  
1000 thank Brandon Wei, Mimi La-Vu, Christopher Lee for experimental support, and the members of the Cai  
1001 and Shuman labs for their feedback throughout the duration of the project. We would like to thank Dr.  
1002 Daniel Aharoni and Federico Sangiuliano Jimka for Miniscope-related support. We thank Dr. Margot  
1003 Tirole, Dr. Claudia Clopath, Geoffroy Delamare, and Sima Rabinowitz for thoughtful discussions and  
1004 input regarding analyses. We thank Dr. Patrick Davis for discussions throughout the project and for  
1005 comments on the manuscript. We thank Stellate Communications for graphical design assistance. We  
1006 thank William Janssen for microscopy support.

1007

1008

1009 **Author Contributions**

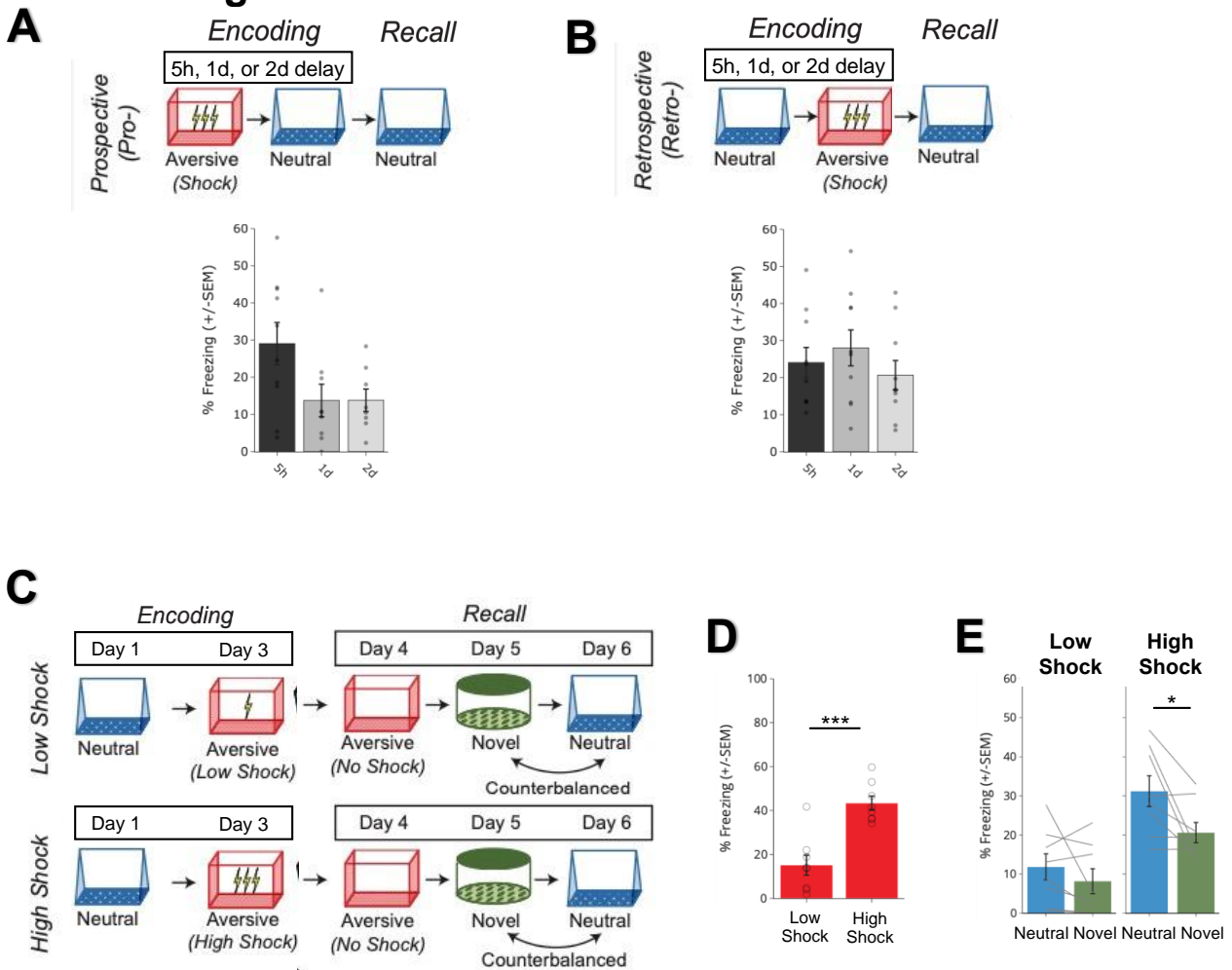
1010 DJC conceived the study. YZ, ZP, DMR, TF, TS, and DJC designed experiments. YZ, ZP, DMR, TF,  
1011 AL, SL, and ZCW conducted behavioral experiments. YZ conducted calcium imaging experiments. YZ,  
1012 DMR, TF, SL, and ZCW conducted chemogenetic experiments. YZ and DJC analyzed data. ZD and ZP  
1013 contributed to development of data processing algorithms. YZ, ZP, DMR, TF, AL, ZD, SCS, HC, AJS,  
1014 Mv, TS, AF, KR, and DJC contributed to interpretation of results. YZ and DJC wrote the manuscript.  
1015 YZ, ZP, DMR, TF, AL, ZD, ZCW, SCS, HC, AJS, Mv, TS, AF, KR, and DJC edited the manuscript.

1016

1017 **Competing Interests**

1018 The authors declare no competing interests.

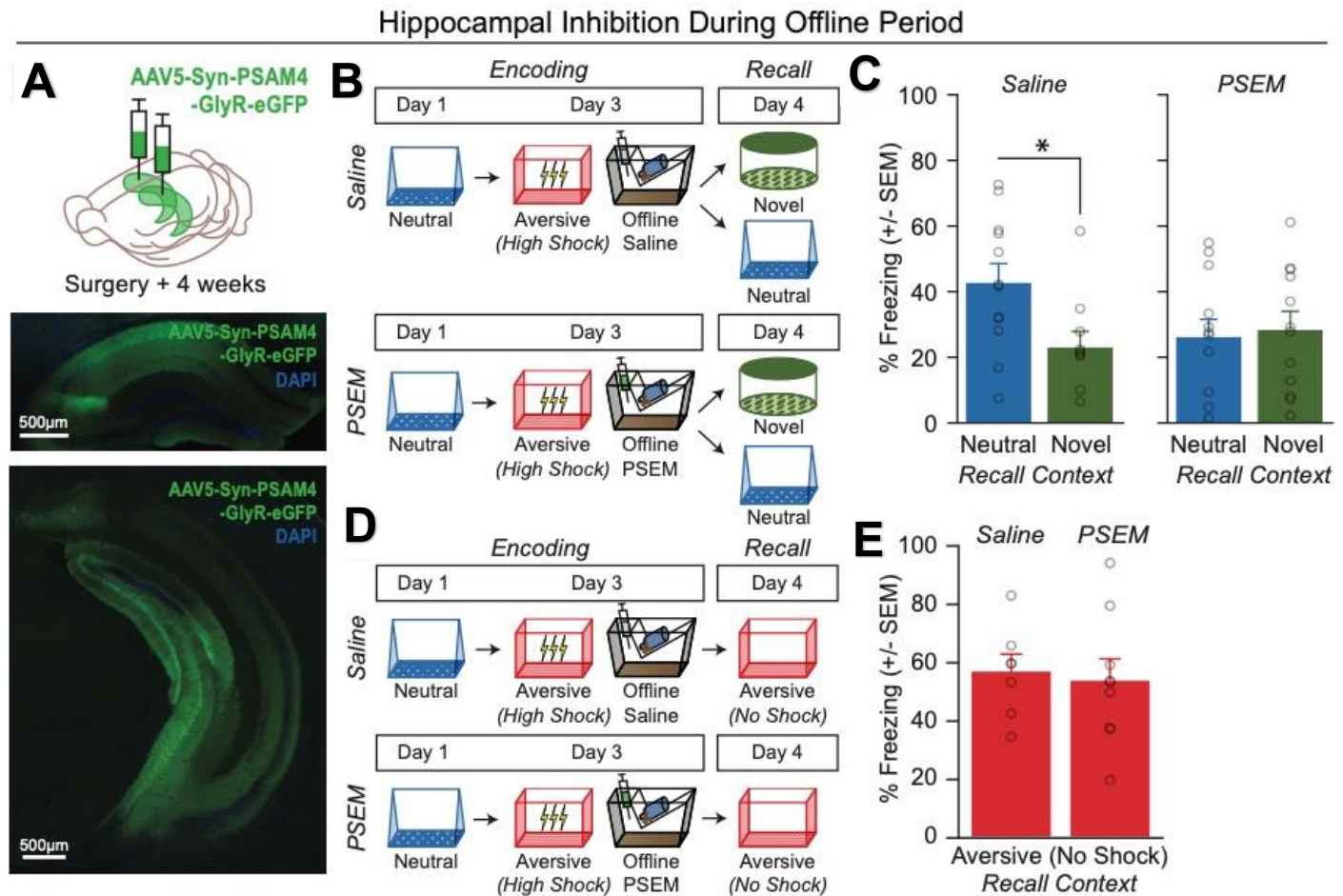
1019 **Extended Figure 1**



1020 **Extended Figure 1. Behavioral experiment controls.**

1021  
 1022 A) Schematic to test the timecourse of prospective memory-linking (top). Mice underwent Aversive encoding and  
 1023 then either 5h, 1d, or 2d later they underwent Neutral encoding. The following day, mice were tested in the  
 1024 previously experienced Neutral context. Mice froze significantly more in the Neutral context when the Neutral  
 1025 context occurred within 5h of the Aversive context, compared to when it occurred one day or more after Aversive  
 1026 encoding (bottom). Main effect of timepoint ( $F_{2,24} = 3.689, p = 0.04$ ) (5h,  $N = 10$  mice; 1d,  $N = 9$  mice; 2d,  $N = 8$   
 1027 mice). Post-hoc tests revealed a trend for higher freezing in the 5h timepoint compared to the 1d or 2d timepoints:  
 1028 1d ( $t_{16.38} = 2.137, p = 0.07$ ), 2d ( $t_{13.45} = 2.38, p = 0.07$ ).  
 1029  
 1030 B) Schematic to test the timecourse of retrospective memory-linking (top). Mice underwent Neutral encoding,  
 1031 followed by Aversive encoding in a separate context 5h, 1d, or 2d later. The day following Aversive encoding, they  
 1032 were tested in the previously experienced Neutral context. Mice froze no differently in the Neutral context  
 1033 regardless of how long before Aversive encoding the Neutral context was experienced (bottom). No main effect of  
 1034 timepoint ( $F_{2,27} = 0.73, p = 0.49$ ) (5h,  $N = 10$  mice; 1d,  $N = 10$  mice; 2d,  $N = 10$  mice).  
 1035  
 1036 C) Schematic of low vs high shock retrospective memory-linking experiment (without calcium imaging as a  
 1037 replication). Mice underwent Neutral encoding followed by a low or high shock Aversive encoding two days later.  
 1038 In the subsequent 3 days, mice were tested in the Aversive context, and then Neutral and Novel contexts,  
 1039 counterbalanced.  
 1040  
 1041 D) Mice froze more in the Aversive context in High Shock vs Low Shock mice ( $t_{14} = 5.04, p = 0.00018$ ) (Low  
 1042 Shock,  $N = 8$  mice; High Shock,  $N = 8$  mice).  
 1043  
 1044 E) High Shock mice exhibited higher freezing in Neutral vs Novel recall, while Low Shock mice did not. A priori  
 1045 post-hoc test: High Shock ( $t_7 = 2.65, p = 0.033$ ), Low Shock ( $t_7 = 1.21, p = 0.133$ ) (Low Shock,  $N = 8$  mice; High  
 1046 Shock  $N = 8$  mice).

## 1047 Extended Figure 2



### 1048 Extended Figure 2. Offline hippocampal activity is necessary to drive retrospective memory-linking

1049  
1050 A) Representative histological verification of viral expression in dorsal and ventral hippocampus. Blue represents  
1051 DAPI and green represents AAV5-Syn-PSAM-GFP.  
1052

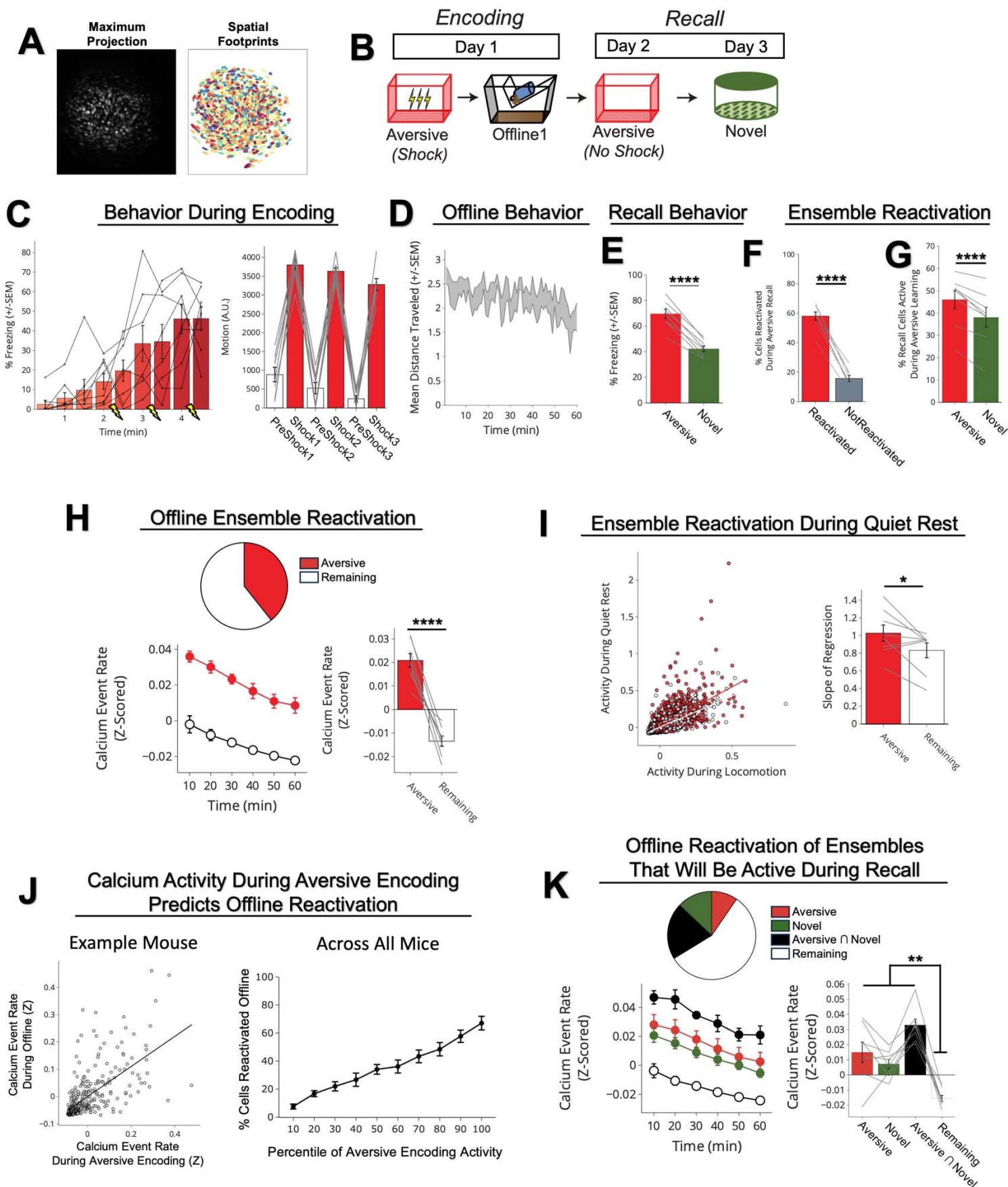
1053 B) Schematic of the behavioral experiment disrupting hippocampal activity during the offline period. Mice were  
1054 injected with AAV5-Syn-PSAM-GFP into dorsal and ventral hippocampus. Mice all had a Neutral experience and  
1055 two days later a strong Aversive experience. Right after Aversive encoding, mice either had the hippocampus  
1056 inactivated for 12hrs using the PSAM agonist, PSEM, or were given saline as a control. To do this, mice were  
1057 injected four times, every three hours, to extend the manipulation across a 12-hour period. Two days later, mice  
1058 were tested in the Neutral or a Novel context for freezing.  
1059

1060 C) Control (saline-treated) mice displayed retrospective memory-linking (i.e., higher freezing during Neutral vs  
1061 Novel recall), while mice that received hippocampal inhibition (PSEM-treated) no longer displayed retrospective  
1062 memory-linking. Significant interaction between Experimental Group (PSEM vs Sal) and Context (Neutral vs  
1063 Novel) ( $F_{1,42} = 4.00, p = 0.05$ ) (Saline Neutral,  $N = 12$  mice; Saline Novel,  $N = 10$  mice; PSEM Neutral,  $N = 12$   
1064 mice; PSEM Novel,  $N = 12$  mice). Post-hoc tests demonstrate higher freezing in Neutral vs Novel contexts in the  
1065 Sal group ( $t_{19,84} = 2.57, p = 0.03$ ) and no difference in freezing in Neutral vs Novel contexts in the PSEM group ( $t_{22}$   
1066  $= 0.31, p = 0.76$ ).  
1067

1068 D) Schematic of the behavioral experiment as above, but this time to test the effects of hippocampal inactivation  
1069 on Aversive memory recall. Mice all underwent the Neutral and Aversive experiences as before, as well as PSEM  
1070 or saline injections following Aversive encoding (as in Extended Figure 2B); however, two days following Aversive  
1071 encoding, mice were tested in the Aversive context to test for an intact aversive memory.  
1072

1073 E) Mice froze no differently in the Aversive context whether they had received hippocampal inhibition or not ( $t_{13,9} =$   
1074  $0.32, p = 0.748$ ) (Saline,  $N = 7$  mice; PSEM,  $N = 9$  mice).

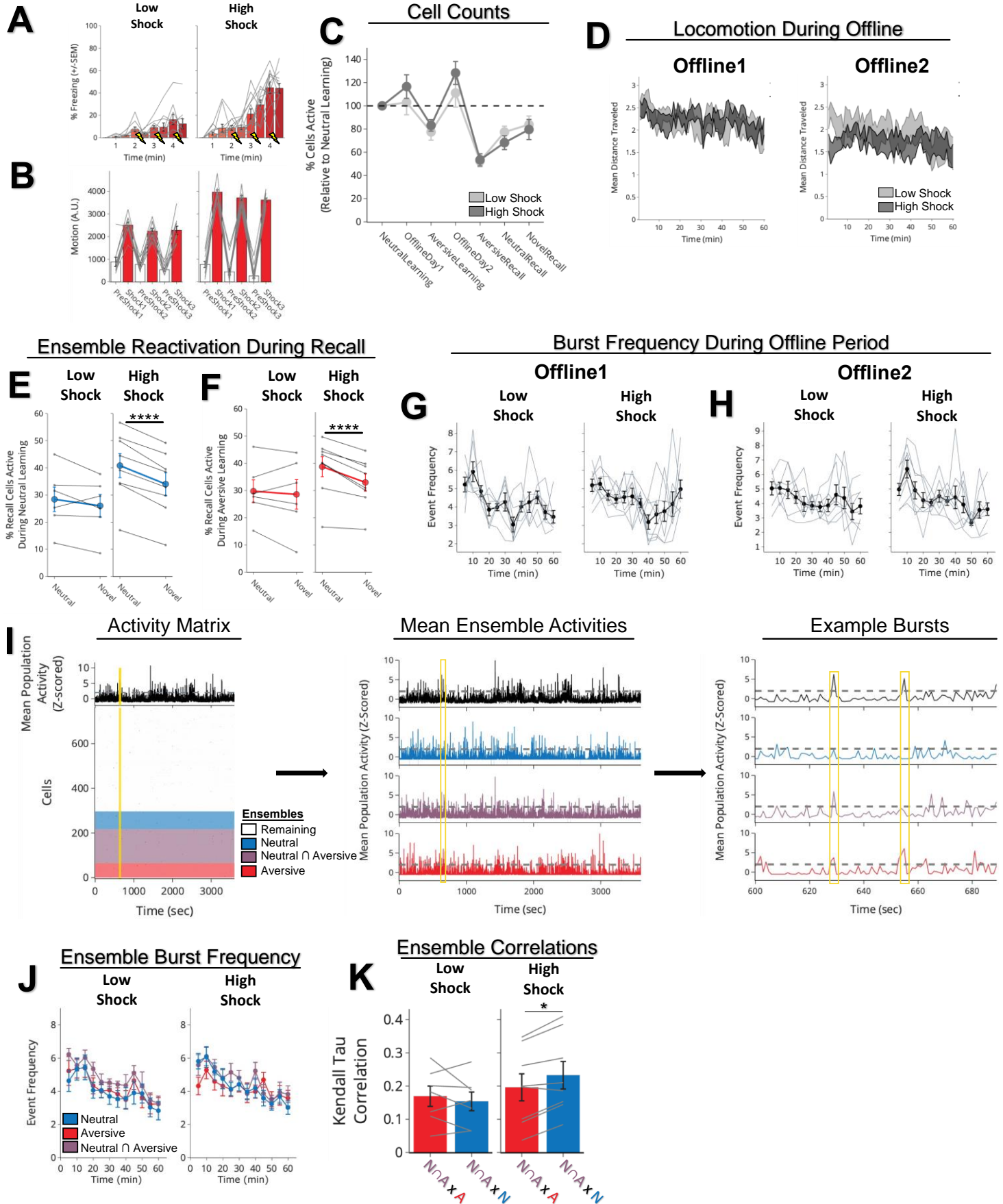
## 1075 Extended Figure 3



1076 **Extended Figure 3. Neurons active during Aversive encoding are selectively reactivated offline and during**  
1077 **Aversive recall.**  
1078  
1079 A) Representative maximum intensity projection of the field-of-view of one example session (left). Spatial  
1080 footprints of all recorded cells during the session, randomly color-coded (right).  
1081  
1082 B) Schematic of a single aversive experience. Mice had an Aversive experience followed by a 1hr offline session  
1083 in the homecage. The next day, mice were tested in the Aversive context, followed by a test in a Novel context  
1084 one day later. Calcium imaging in hippocampal CA1 was performed during all sessions.  
1085  
1086 C) Mice acquired within-session freezing during Aversive encoding (left); main effect of time ( $F_{8,56} = 12.59$ ,  $p =$   
1087  $3.87e-10$ ,  $N = 8$  mice). And mice responded robustly to all three foot shocks, though their locomotion generally  
1088 decreased across shocks, driven by increased freezing (right); main effect of shock number ( $F_{2,14} = 7.45$ ,  $p =$   
1089  $0.0154$ ,  $N = 8$  mice) and main effect of PreShock vs Shock ( $F_{1,7} = 581$ ,  $p = 5.38e-8$ ,  $N = 8$  mice), and no  
1090 interaction.  
1091  
1092 D) Mice displayed a modest decrease in locomotion across the 1hr offline period ( $R^2 = 0.064$ ,  $p = 1.9e-8$ ,  $N = 8$   
1093 mice).  
1094  
1095 E) Mice froze significantly more in the Aversive context than in a Novel context during recall ( $t_7 = 165$ ,  $p = 4e-6$ ,  $N = 8$   
1096 mice).  
1097  
1098 F) Cells that were active during Aversive encoding and reactivated offline were significantly more likely to be  
1099 reactivated during Aversive recall than cells active during Aversive encoding and not reactivated offline ( $t_7 =$   
1100  $19.41$ ,  $p = 2e-7$ ,  $N = 8$  mice).  
1101  
1102 G) A larger fraction of cells active during Aversive recall than during Novel recall were previously active during  
1103 Aversive encoding ( $t_7 = 6.897$ ,  $p = 0.0002$ ,  $N = 8$  mice).  
1104  
1105 H) During the offline period, ~40% of the population was made up of cells previously active during Aversive  
1106 encoding (top). This Aversive ensemble was much more highly active than the rest of the population during the  
1107 offline period (bottom; A.U.) ( $t_7 = 8.538$ ,  $p = 0.00006$ ,  $N = 8$  mice).  
1108  
1109 I) Each cell's activity was compared during locomotion vs during quiet rest (left; A.U.). A regression line was fit to  
1110 the cells in the Aversive ensemble and in the Remaining ensemble separately, for each mouse. The Remaining  
1111 ensemble showed greater activity during locomotion than during quiet rest (i.e., a less positive slope). The  
1112 Aversive ensemble showed relatively greater activity during quiet rest than locomotion (i.e., a more positive slope)  
1113 across mice (right) ( $t_7 = 5.76$ ,  $p = 0.047$ ,  $N = 8$  mice).  
1114  
1115 J) Cells that had high levels of activity (A.U.) during Aversive encoding continued to have high levels of activity  
1116 during the offline period (example mouse; left). There was a linear relationship between how active a cell was  
1117 during Aversive encoding and how likely it was to be reactivated during the offline period (all mice; right) ( $R^2 =$   
1118  $0.726$ ,  $p = 1.25e-23$ ,  $N = 8$  mice).  
1119  
1120 K) During the offline period, cells that would go on to become active during recall were more highly active than the  
1121 Remaining ensemble during the offline period. The top represents the proportion of each ensemble (legend to its  
1122 right). The cells that would become active during both Aversive and Novel recall were most highly active (A.U.).  
1123 There was no difference in activity in the cells that would go on to be active in Aversive or Novel. Main effect of  
1124 Ensemble ( $F_{3,21} = 27.81$ ,  $p = 1.65e-7$ ,  $N = 8$  mice). Post-hoc tests: for Aversive vs Novel ( $t_7 = 1.33$ ,  $p = 0.22$ ), for  
1125 Remaining vs Aversive  $\cap$  Novel ( $t_7 = 11.95$ ,  $p = 0.000007$ ), for Remaining vs Aversive ( $t_7 = 3.97$ ,  $p = 0.005$ ), for  
1126 Remaining vs Novel ( $t_7 = 7.47$ ,  $p = 0.0001$ ).

# 1127 Extended Figure 4

## Aversive Encoding Behavior



#### 1128 **Extended Figure 4. Low vs High Shock calcium imaging supplementary analyses.**

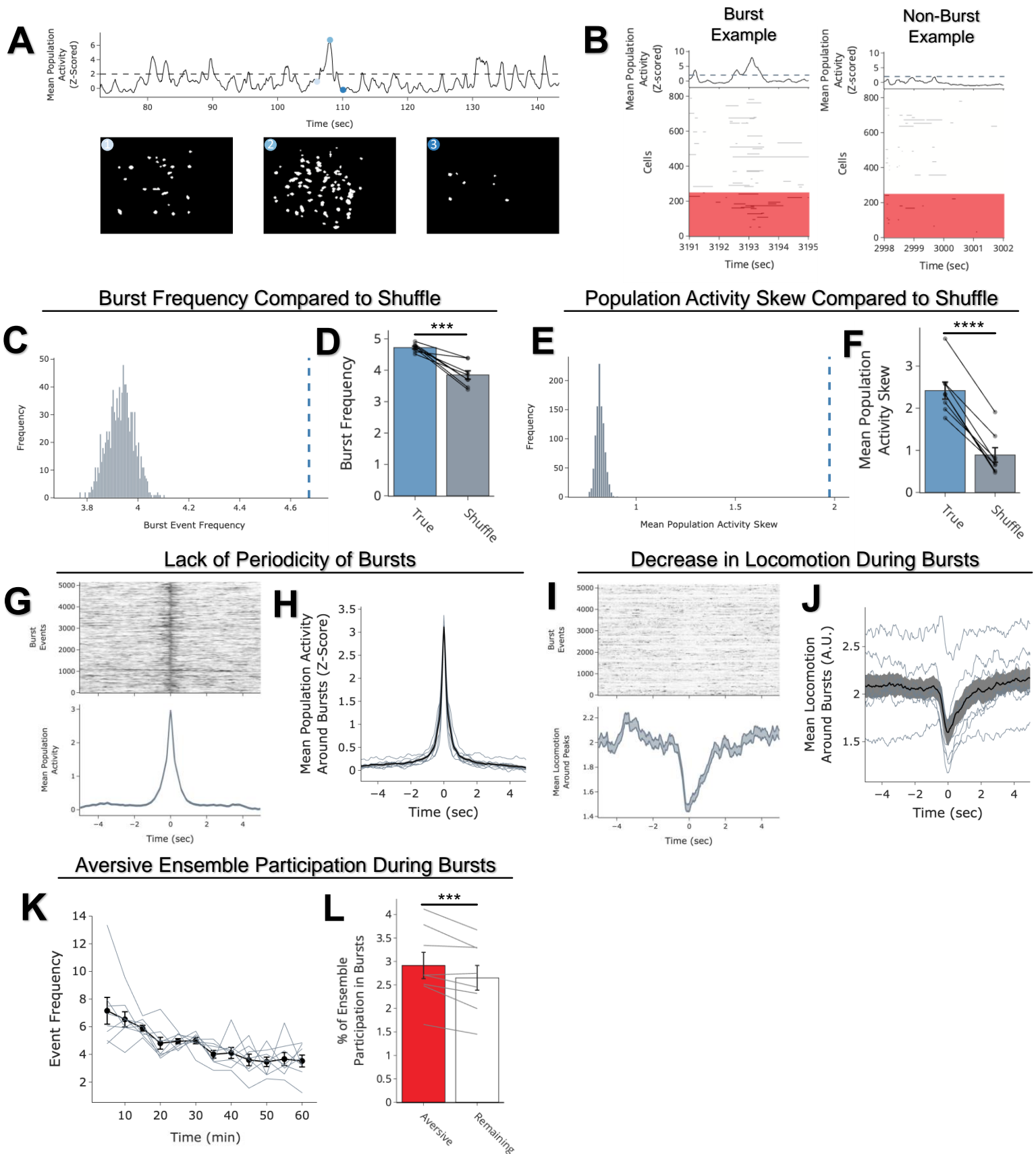
- 1129
- 1130 A) Mice acquired within-session freezing during Aversive encoding. Mice that received high shocks (1.5mA)
- 1131 displayed more freezing than mice that received low shocks (0.25mA) (*Low Shock, N = 10 mice; High Shock, N =*
- 1132 *12 mice*).
- 1133
- 1134 B) Mice responded robustly to each foot shock. High shock mice responded more strongly to each shock than low
- 1135 mice did (*Low Shock, N = 10 mice; High Shock, N = 12 mice*).
- 1136
- 1137 C) Relative to the first calcium imaging recording, mice showed comparable fractions of observed cells across the
- 1138 remaining sessions (*Low Shock, N = 8 mice; High Shock, N = 10 mice*).
- 1139
- 1140 D) Locomotion across the 1hr offline period after Neutral encoding (Offline1) and after Aversive encoding
- 1141 (Offline2) in Low and High Shock mice. Mice showed decreased locomotion across the offline period on both
- 1142 days. Low Shock mice did not locomote differently from High Shock mice during either offline period (*Low Shock,*
- 1143 *N = 10 mice; High Shock, N = 12 mice*).
- 1144
- 1145 E) In High Shock mice, Neutral recall cells were composed of more Neutral encoding cells being reactivated,
- 1146 compared to Novel recall cells. In Low Shock mice, Neutral recall cells and Novel recall cells were composed of
- 1147 similar fractions of Neutral encoding cells being reactivated. Significant interaction between Context (Neutral vs
- 1148 Novel) and Amplitude (Low vs High Shock) ( $F_{1,12} = 6.81, p = 0.022$ ) (*Low Shock, N = 6 mice; High Shock, N = 8*
- 1149 *mice*). Post-hoc tests, *Low Shock* ( $t_5 = 1.34, p = 0.24$ ), *High Shock* ( $t_7 = 10.22, p = 0.000037$ ).
- 1150
- 1151 F) In High Shock mice, Neutral recall cells were composed of more Aversive encoding cells being reactivated,
- 1152 compared to Novel recall cells. In Low Shock mice, Neutral recall cells and Novel recall cells were composed of
- 1153 similar fractions of Aversive encoding cells being reactivated. Significant interaction between Context (Neutral vs
- 1154 Novel) and Amplitude (Low vs High Shock) ( $F_{1,12} = 4.75, p = 0.0499$ ) (*Low Shock, N = 6 mice; High Shock, N = 8*
- 1155 *mice*). Post-hoc tests, *Low Shock* ( $t_5 = 0.59, p = 0.58$ ), *High Shock* ( $t_7 = 5.46, p = 0.0019$ ).
- 1156
- 1157 G) During Offline1, burst event frequency gradually decreased across the hour ( $F_{11,143} = 4.43, p = 1.0e-5$ ). No
- 1158 difference across shock amplitudes ( $F_{11,13} = 0.31, p = 0.587$ ) (*Low Shock, N = 7 mice; High Shock, N = 8 mice*).
- 1159 Significant interaction between Time and Amplitude ( $F_{11,143} = 1.87, p = 0.047$ ). Follow-up repeated measures
- 1160 ANOVAs showed that both Low and High Shock groups showed a significant decrease in event rate across time
- 1161 (*Low Shock: F*<sub>11,66</sub> *= 4.13, p = 0.0001; High Shock: F*<sub>11,77</sub> *= 2.43, p = 0.01*).
- 1162
- 1163 H) During Offline2, burst event frequency decreased across time ( $F_{11,143} = 6.69, p = 0.000054$ ). No difference
- 1164 across shock amplitudes ( $F_{1,13} = 0.0056, p = 0.94$ ) (*Low Shock, N = 7 mice; High Shock, N = 8 mice*).
- 1165
- 1166 I) Example process of identifying ensemble co-participations during bursts. Data in this panel are down-sampled
- 1167 from 30Hz to 1Hz for visualization purposes. On the left, the bottom matrix represents the neuronal activities for
- 1168 all neurons recorded across the offline period, color-coded by ensemble (see Ensembles legend). The top black
- 1169 trace represents the z-scored mean population activity across the hour. The yellow line represents a time slice of
- 1170 representative bursts (expanded on the right). In the middle, the whole population mean population activity is
- 1171 shown again, with the mean population activity of the Neutral, Neutral  $\cap$  Aversive, and Aversive ensembles
- 1172 shown below. From these population activities, the time periods above threshold for the whole population were
- 1173 considered whole population bursts, and within those, we measured how frequently the other ensembles
- 1174 participated in these bursts. On the right, we zoom into two example whole population bursts in yellow. In the first
- 1175 one, at 629 sec into the recording, the Neutral  $\cap$  Aversive and Aversive ensembles participated, and in the
- 1176 second one, at 655 sec, only the Aversive ensemble participated.
- 1177
- 1178 J) During Offline2, bursts as defined by each ensemble (rather than by whole population) decreased across the
- 1179 hour, with comparable frequencies across ensembles and amplitudes (*Low Shock, N = 7 mice; High Shock, N = 8*
- 1180 *mice*).
- 1181
- 1182 K) Time-lagged cross correlations between the N $\cap$ A ensemble and the Neutral and Aversive ensembles during
- 1183 the offline period. Each of the three ensembles (N $\cap$ A, Neutral, and Aversive) were binned into 120 sec bins. Each
- 1184 time bin of N $\cap$ A ensemble activity was cross-correlated with the corresponding time bin of Neutral ensemble and
- 1185 Aversive ensemble activity. Cross-correlations were computed with a maximum time lag of 5 frames (or, ~160ms).
- 1186 For each mouse, the correlations were averaged across all time bins to get an average cross-correlation between
- 1187 the N $\cap$ A ensemble and Neutral ensemble (i.e., N $\cap$ A x N) and the N $\cap$ A ensemble by Aversive ensemble (i.e.,
- 1188 N $\cap$ A x A). There was a significant interaction between Ensemble Combination and Low vs High Shock group

1189 ( $F_{1,13} = 6.70, p = 0.02$ ) (*Low Shock, N = 7 mice; High Shock, N = 8 mice*). Post-hoc tests revealed that in High  
1190 Shock mice, N∩A x N correlations were higher than N∩A x A correlations ( $t_7 = 3.97, p = 0.01$ ) whereas they were  
1191 no different in Low Shock mice ( $t_6 = 0.83, p = 0.44$ ).



# 1192 Extended Figure 5

## Burst Classification



1193 **Extended Figure 5. Neurons active during Aversive encoding selectively participate in burst events**  
1194 **offline.**  
1195

1196 A) Example of a burst event quantified in this figure. The top trace represents the z-scored mean population  
1197 activity within one of the offline recordings. Three timepoints were chosen (overlaid in circles), the middle  
1198 representing the peak of a burst event, and the timepoints to its left and right representing t-2sec and t+2sec from  
1199 the peak, respectively. The bottom three matrices represent binarized spatial footprints depicting the spatial  
1200 footprints of the cells sufficiently active to participate in a burst ( $z > 2$ ). The matrices represent the timepoints of the  
1201 three datapoints above it, ordered by time.  
1202

1203 B) Representative process of extracting ensemble participations (one mouse example). The left is an example  
1204 burst period, with the rows in the heatmap representing the activity of the recorded cells during that session,  
1205 binarized by  $z > 2$  and color-coded by whether they were previously active during Aversive encoding (Aversive  
1206 ensemble, blue) or if they were not previously active (Remaining ensemble, grey). The black trace above  
1207 represents the z-scored mean population activity during this period, demonstrating a brief burst in activity  
1208 accompanied by participation by a significant fraction of neurons. On the right is an example non-burst period,  
1209 where mean population activity remains below threshold.  
1210

1211 C) Neuron activities were circularly shuffled 1000 times relative to one another and the mean population activity  
1212 was re-computed each time. This shuffling method preserved the autocorrelations for each neuron while  
1213 disrupting the co-firing relationships between neurons. The burst frequency was computed for each of these  
1214 shuffles to produce a shuffled burst frequency distribution (gray histogram), to which the true burst frequency was  
1215 compared (blue dotted line). This is an example mouse.  
1216

1217 D) The mean burst frequency for the shuffled distribution was computed and compared to the true burst frequency  
1218 for each mouse. True burst frequencies were greater than shuffled burst frequencies in every mouse ( $t_7 = 6.159$ ,  $p$   
1219  $= 0.000463$ ,  $N = 8$  mice), suggesting that during the offline period, hippocampal CA1 neurons fire in a more  
1220 coordinated manner than would be expected from shuffled neuronal activities.  
1221

1222 E) As in Extended Figure 5C, neuron activities were shuffled, and mean population was re-computed each time.  
1223 From this population activity trace, the skew of the distribution was computed. If there were distinct periods where  
1224 many neurons simultaneously fired, we hypothesized that the true distribution of mean population activity would  
1225 be more skewed with a strong right tail demonstrating large and brief deflections, compared to shuffled neuronal  
1226 activities. We computed the skew of each shuffled mean population activity, to produce a distribution (gray  
1227 histogram), to which the true mean population's skew was compared (blue dotted line). This is an example  
1228 mouse.  
1229

1230 F) The mean skew for the shuffled distribution was computed and compared to the true skew of the mean  
1231 population activity for each mouse. The true skew was greater than the shuffled skew in every mouse ( $t_7 = 13.36$ ,  
1232  $p = 0.000003$ ,  $N = 8$  mice), supporting the idea that the mean population activity undergoes brief burst-like  
1233 activations requiring the coordinated activity of groups of neurons.  
1234

1235 G) Matrix of burst events for an example mouse, stacked along the y-axis and centered on time t=0 (top), and the  
1236 average mean population activity around each burst event (bottom).  
1237

1238 H) As in Extended Figure 5G but averaged across all mice. Each thin line represents one mouse, and the thick  
1239 black line represents the mean across mice with the grey ribbon around it representing the standard error ( $N = 8$   
1240 mice). There is no periodicity to when these burst events occur.  
1241

1242 I) Locomotion of an example mouse during each burst event stacked along the y-axis (top), and the mean  
1243 locomotion around burst events (bottom). Mice showed a robust and brief slowing down ~1sec before each burst  
1244 event, before increasing locomotion back up ~2sec later.  
1245

1246 J) As in Extended Figure 5I but averaged across all mice. Each thin line represents one mouse, and the thick  
1247 black line represents the mean across mice with the grey ribbon around it representing the standard error ( $N = 8$   
1248 mice). This demonstrates a robust and reliable decrease in locomotion around the onset of burst events.  
1249

1250 K) The burst event frequency decreased across the hour ( $F_{11,77} = 6.91$ ,  $p = 5.66e-8$ ,  $N = 8$  mice).  
1251

1252 L) A larger fraction of the Aversive ensemble vs the Remaining ensemble participated in each burst event (left) ( $t_7$   
1253  $= 3.68$ ,  $p = 0.0079$ ,  $N = 8$  mice).